



BOREHOLE GEOLOGY AND HYDROTHERMAL MINERALISATION OF WELL OW-916, OLKARIA DOMES GEOTHERMAL FIELD, NAIVASHA, KENYA

David Wanjohi Mwangi

Kenya Electricity Generating Company – KenGen

P.O. Box 785 – 20117

Naivasha

KENYA

dwanjohi@kengen.co.ke

ABSTRACT

Well OW-916 is one of the production wells located in the Olkaria Domes Geothermal field in Naivasha, Kenya. The well is vertical. A geological analysis from the surface to 3000 m depth is presented in this report. Comprehensive binocular and petrographic analyses indicate that the lithology of the well is comprised of five different formations and minor intrusive rocks. These formations/units host secondary hydrothermal mineral assemblages which are dependent on temperature, permeability and rock type, and they show evolution of the hydrothermal system from low- to high-temperature conditions with depth, as observed from alteration minerals in veins and vesicles. The relationship between depth and hydrothermal mineral formation indicates low-temperature minerals at shallow depths and high-temperature minerals at greater depths. Three alteration zones were identified: a zeolite-illite zone, an epidote-chlorite-illite zone and an actinolite-epidote-chlorite-illite zone. Several feed zones were encountered and classified into major and minor feed zones, and they are associated with fractures, lithological contacts and circulation losses encountered during drilling. The larger feed zones are between 650 and 1300 m and they show little cooling when comparing the alteration and formation temperatures. Fluid inclusion analyses indicate that the system is in equilibrium since the homogenisation temperatures of the inclusions are close to the current measured formation temperature of the well. Alteration and formation temperatures, however, indicate that the past geothermal conditions were at higher temperatures than current conditions. A comparison with other wells drilled in this area shows similarities in the lithology but alteration mineralogy shows that, in this well, alteration is high between 600 and 1500 m. The well produces 16 MW and epidote and actinolite are observed at shallower depth in this well than in the three other wells in this field to which it was compared, indicating that this area might be a possible up flow zone. The comparison also stresses the role and importance of temperature in all geothermal systems.

1. INTRODUCTION

1.1 General information

The Olkaria geothermal field (Figure 1) is one of the largest geothermal fields in Kenya. The field is located within the Greater Olkaria Volcanic Complex (GOVC) in the central sector of the Kenya Rift Valley to the south of Lake Naivasha and 120 km from Nairobi, the capital city of Kenya. Olkaria is a high-temperature geothermal system, with reservoir temperatures above 200°C.

Exploration for geothermal resources in Kenya began in GOVC in 1956, when two wells, X-1 and X-2, were drilled (Kenya Power Company, 1984) and high temperatures were encountered at shallow depth. Further exploration in the area commenced in 1970 through bilateral and multilateral agreements between UNDP (United Nations Development Programme) and the Government of Kenya. Drilling recommenced with well OW-1 in 1973. Although the well intersected low temperatures, subsequent drilling 3 km northeast of the well site (OW-2) confirmed the existence of a high-temperature hydrothermal system, and further drilling was confined to this area, which is the current Olkaria East production field.

The Olkaria geothermal field is divided into seven smaller fields, namely: Olkaria East, Olkaria Northeast, Olkaria Central, Olkaria Northwest, Olkaria Southwest, Olkaria Southeast and Olkaria Domes. The Olkaria East field (Olkaria I) has been producing power since 1981 and currently produces 45 MW. The Northeast field (Olkaria II) has a plant which opened in 2003 and produces 105 MW, while Olkaria Northwest field, owned by OrPower, an independent power producer, generates 48 MW.

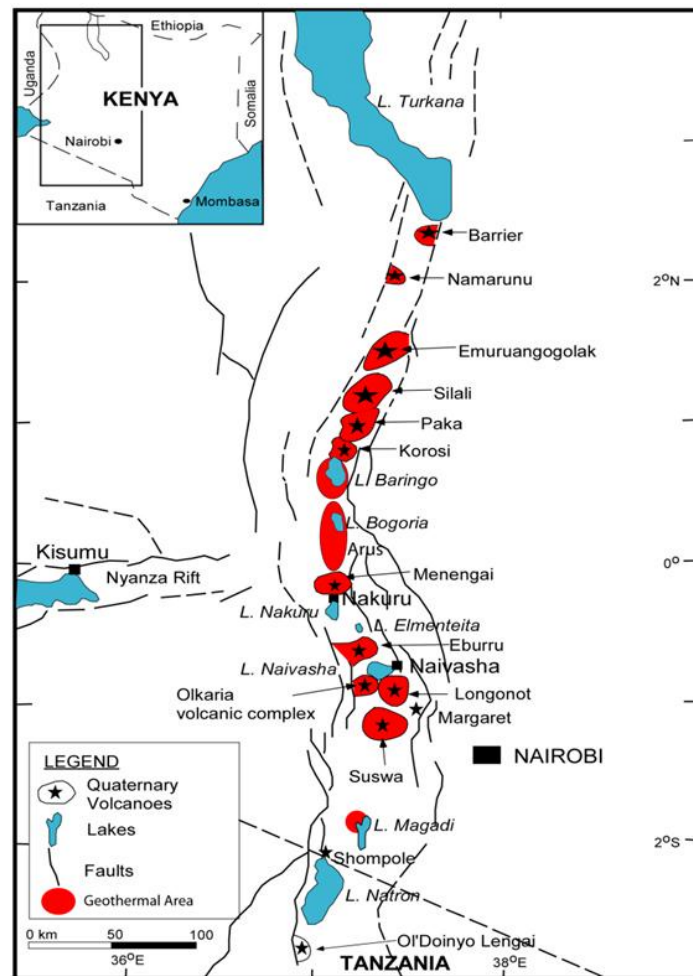


FIGURE 1: Location of Olkaria geothermal field (Ofwona et al., 2006)

Currently, two plants are under construction, an additional 140 MW plant in the Olkaria East field and a 140 MW plant in the Olkaria Domes field. Together the plants will add 280 MW to the power grid.

Well OW-916 is one of 25 production wells that have been drilled in the Olkaria Domes since 1998 in an effort to meet the increasing demand for electricity in Kenya. OW-916 is a vertical well drilled to 3000 m measured depth and this geological report describes the geology of the well, including the lithology, hydrothermal mineralisation, sequences of mineral deposition, and aquifers.

The study presented here is carried out as a requirement of partial fulfilment of the United Nations University Geothermal Training Programme six month course in the year 2012.

2. GEOLOGICAL AND STRUCTURAL SETTINGS

2.1 Regional geology

Olkaria is located in the Kenya Rift Valley, which is part of the East African Rift System. The Kenyan Rift is situated on a divergent plate boundary, where the Somali and Nubian plates are drifting apart at a rate of about 2 cm per year, thus creating a thinner crust (KenGen, 1998). The rift formation began in the early Miocene in the north around Lake Turkana (Figure 2) and propagated southwards, being active from about middle to late Miocene in the central segment (Omenda, 1998).

Rift tectonics has resulted in intense volcanism in the rift; numerous central volcanoes of Quaternary age were formed, and they are predominantly silicic in composition. These volcanoes are built largely of intermediate lavas and associated pyroclastics, indicating the presence of shallow hot bodies and active magmatism under the rift.

Geothermal manifestations like fumaroles, hot springs, hot and altered grounds are more abundant and stronger within the rift and most of them are associated with the young quaternary volcanoes (Omenda, 1998). Thinning of the crust in the rift is also responsible for the general high heat flow within the rift, with a geothermal gradient of over 200°C/km (Wheildon et al., 1994). The southern part of the Kenyan Rift Valley has at least four Quaternary to Recent volcanic complexes which include Suswa, Longonot, Olkaria and Eburru (Lagat, 2004).

2.2 Geological evolution of Olkaria

The Greater Olkaria volcanic complex (GOVC) in the South Central Kenya Rift Valley is a young, small-volume, frequently-erupting, multi-centred system dominated at outcrops by peralkaline rhyolite domes and lava fields (Marshall et al., 2009). It is part of the Central Kenya Peralkaline Province (CKPP) (MacDonald and Scaillet, 2006) which coincides with an area of crustal upwarping known as the Kenya Dome (Baker and Wohlenberg, 1971).

Petrological studies that were done in this field (Davies and MacDonald, 1987; MacDonald et al., 1987) referred to the GOVC as the Naivasha complex. Clarke et al. (1990) introduced GOVC in order to stress the close association of the rocks

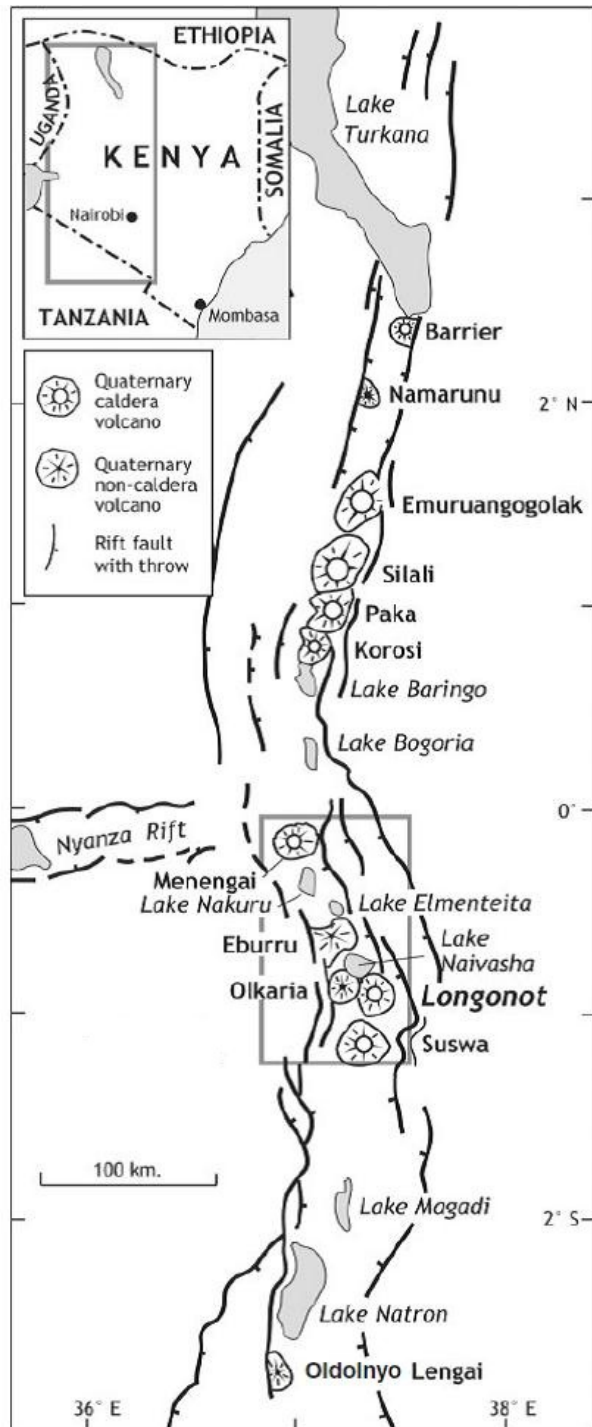


FIGURE 2: Quaternary volcanoes in the Kenyan Rift Valley (Marshall et al., 2009)

with the well-known Olkaria geothermal field. Crustal thickness beneath the dome is 30-35 km (Mechie et al., 1997).

The geological age of GOVC is not fully revealed, but on the basis of its relationship to the age of high stands in the local lakes, Clarke et al. (1990) placed it in the period of Late Pleistocene age, about 22-20 ka BP.

The complex is bounded on the north by the Eburru complex, on the east and south by the Longonot and Suswa volcanoes respectively, and on the west by the western rift margin (Figure 2). At least 80 small volcanic centres have formed in the complex; most occur either as steep-sided domes, formed by lavas and/or pyroclastic rocks, or as thick lava flows of restricted lateral extent (Marshall et al., 2009). The ring structure formed by the domes indicates the presence of a buried caldera. The GOVC (Figure 3) is characterised by comendite lava flows and pyroclastics on the surface and basalts, trachytes, and tuffs in the subsurface (Marshall et al., 2009). Six stages have been recognised in the evolution of this complex:

Stage 1: Pre-caldera magmatism, involving the formation of predominantly trachytic lava and a pumice pile, represented by the Olkaria trachyte formation and the Maiella pumice formation (Macdonald et al., 2008). Pumice is widespread to the west of the complex and is thought to have been erupted from fissures or vents within the complex. The trachyte lavas are exposed mainly in gullies and ridges in the southwest part of the complex.

Stage 2: Using evidence from the well-developed ring structure, the presence of a ring of rhyolite domes, pyroclastic deposits around this structure, apparent resurgent activity within the ring structure and the distribution of the fumaroles, Clarke et al. (1990) argued that the trachytic eruptions were followed by a caldera collapse, which left a large depression of about 82.5 square kilometres. This collapse was accompanied by an eruption of the welded pyroclastic rocks of the Ol Njorowa pantellerite formation, which is now exposed only in the deepest parts of the Ol Njorowa Gorge.

Stage 3: Post-caldera magmatism of the Lower Comendite member of the Olkaria Comendite Formation is represented by rhyolite lavas and pyroclastics, and was dated by the ^{14}C method to have occurred at $>9150 \pm 110$ BP (Figure 4).

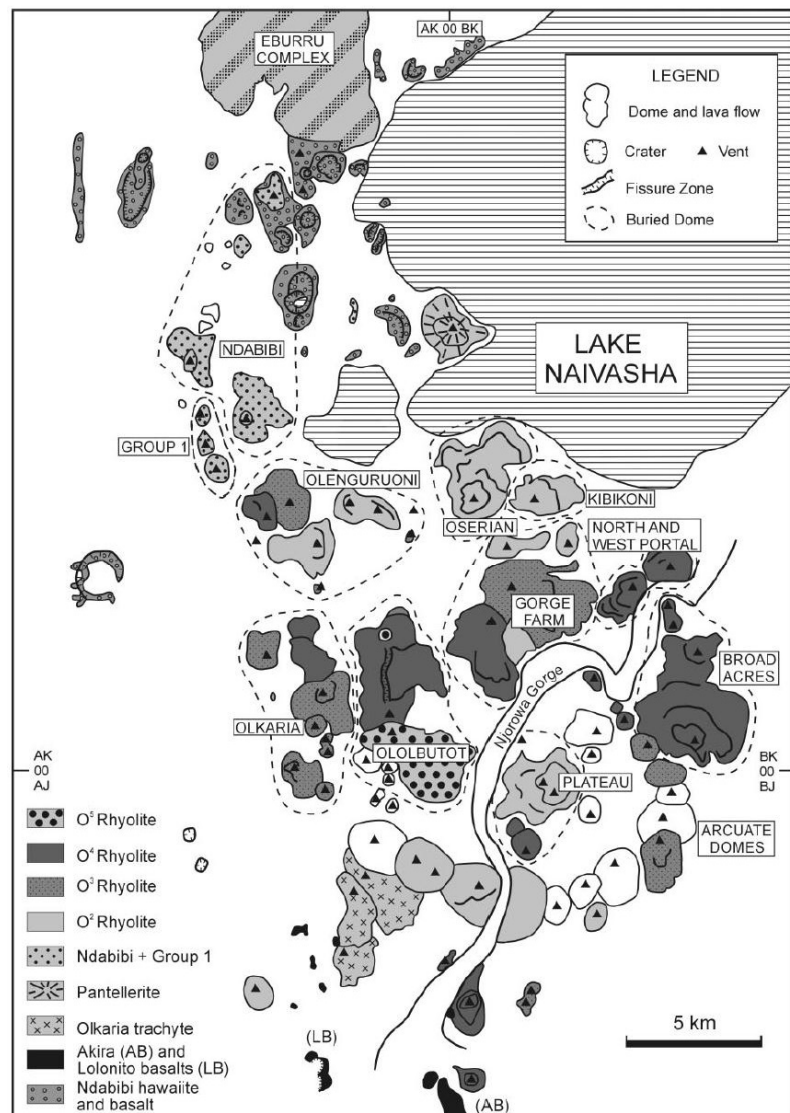


FIGURE 3: Geology of GOVC (Marshall et al., 2009)

Stage 4: The Middle comendite member is a period of ring dome formation, comprised mainly of rhyolitic lavas and the eruption of thick pyroclastic deposits which happened between $>9150 \pm 110$ and $>3280 \pm 120$ BP.

Stage 5: The Upper Comendite member involved a resurgence of the caldera floor and the formation of short, thick lava flows.

Stage 6: Eruptions of very thick lava flows of comendite from a north–south fissure system. The youngest lava flow, Ololbutot comendite, yielded a ^{14}C date of 180 ± 50 BP (Clarke et al., 1990).

Subsurface geology of the wells drilled in the Greater Olkaria Volcanic Complex can be divided into six main rock types: the Proterozoic basement formation, pre Mau volcanics, Mau tuffs, plateau trachytes, Olkaria basalt and upper Olkaria volcanics (Omenda, 2000). The basement formation is not observed in this field but is overlain by the pre Mau volcanics, consisting of basalts and ignimbrites which are of unknown thickness. The Mau tuffs overlie the pre Mau volcanics; they are common in the area west of Olkaria hill but are absent in the east, due to an east dipping high angle fault that passes through Olkaria hill (Omenda, 1994; 1998). The rocks vary in texture from consolidated to ignimbritic and are the main geothermal reservoir rocks in the Olkaria West field, as observed from well cuttings.

Plateau trachytes observed in the wells in Olkaria are part of the Kenyan rift floor and are Pleistocene in age, occurring from about 1000 m to more than 3000 m (Omenda, 1994; 1998). They are mainly composed of trachytes together with minor basalts, tuffs and rhyolites and host the geothermal reservoir in the eastern Olkaria geothermal fields. Olkaria basalt underlies the upper Olkaria volcanics in the area east of Olkaria hill but is absent to the west and consists of basalts with minor pyroclastics and trachytes. The formation, which ranges in thickness from 50 to 500 m, acts as the cap rock for the Olkaria geothermal system (Haukwa, 1984; Ambusso and Ouma, 1991; Omenda, 1998).

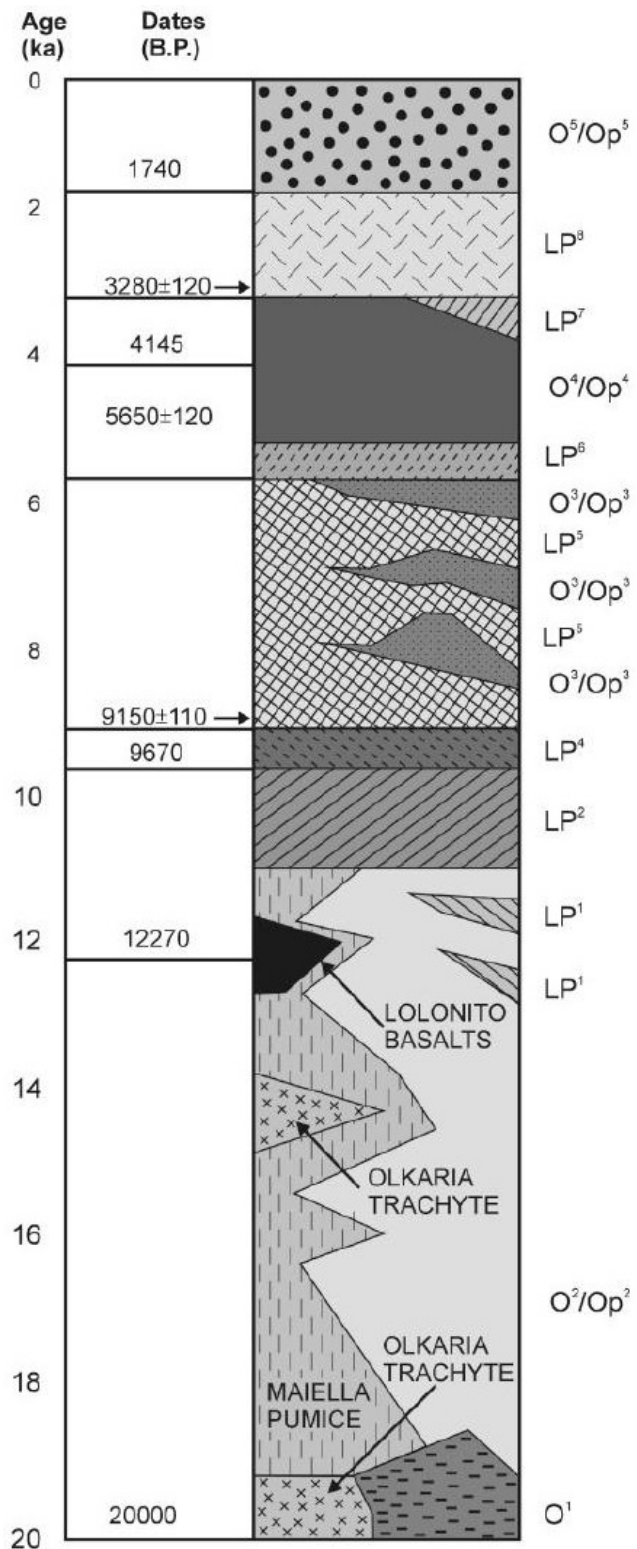


FIGURE 4: Stratigraphic column of the Greater Olkaria volcanic complex (Marshall et al., 2009); units O1 TO O5/OP5 and the Olkaria Trachyte are from the Olkaria Complex while LP1 to LP8 are Longonot Pumice Falls

2.3 Structural setting

The geology and geological structures of Olkaria are described in reports by Thompson and Dodson (1963) and McCall (1967). Naylor (1972) was the first person to document the concept of a ring structure around the volcanic complex in Olkaria, which was supposedly destroyed by an explosive eruption accompanied by a caldera collapse. This activity was then followed by peripheral volcanic activity along the ring structure. Clarke et al. (1990) also suggested that Ol' Njorowa gorge (Figure 5), which cuts the suggested ring structure from north to south, was formed by faulting and catastrophic flooding of Lake Naivasha during its high stands. Volcanic plugs (necks) and felsic dikes which occur along the gorge further attest to the fault control in the development of this feature.

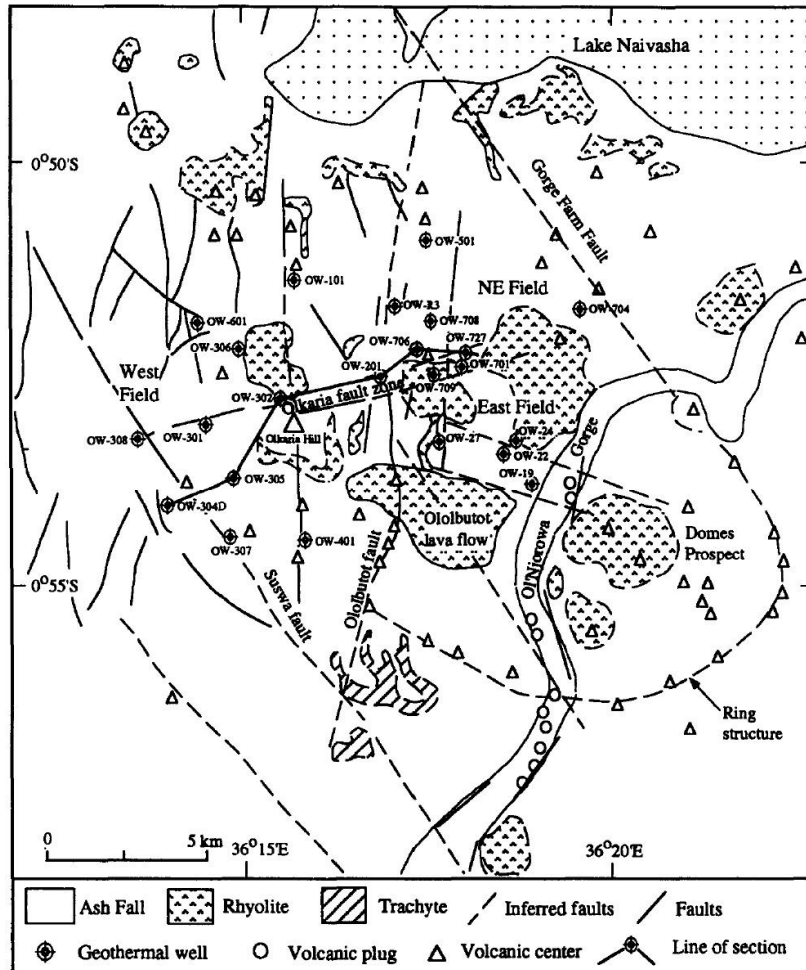


FIGURE 5: Structural map of Olkaria (modif. from Omenda, 1998)

Structures in GOVC include: the ring structure, the Ol' Njorowa gorge, the ENE-WSW Olkaria fault and N-S, NNE-SSW, NW-SE and WNW-ESE trending faults (Lagat, 2004). The main rift faults become more prominent from Olkaria Hill where a NNW-SSE high-angle fault is displayed by the Mau Escarpment (Omenda, 1998). The NW-SE and WNW-ESE faults are thought to be the oldest, with most of them being observed from aerial photos and the alignment of the volcanic centres, and are associated with the development of the Rift Valley. The young N-S faults and fractures are the most common in the axial rift of the rift floor and represent the latest tectonic activity in this area. This pattern is also observed north of Eburru and south of Suswa, where a fault density of more than 3- 5 faults per kilometre is common (Omenda, 1998).

The ENE-WSW trending Olkaria fault, which runs through the Olkaria geothermal area, is interpreted to be an old rejuvenated structure. It is observed on the surface by a linear zone of intense geothermal manifestations and highly altered grounds, about 50-100 m in width. Fumaroles in this area are at boiling point with sulphur and silica deposits observed on the surface. This fault has a surface displacement of about 5 m with a downthrow to the north (Omenda, 1998).

The other prominent fault is the Gorge Farm fault, which bounds the geothermal fields in the north-eastern part of the GOVC and extends to the Olkaria Domes area (Lagat, 2004). Another important structure is the ring structure, which is well represented by the arcuate alignment of the Domes on the eastern part of the GOVC and is thought to indicate the presence of a buried caldera (Naylor, 1972; Clarke et al., 1990; Mungania, 1992).

It has been proposed that the ring structure might have been produced by magmatic stresses in the Olkaria magma chamber, and that the lines of weakness in this structure were responsible for the subsequent rhyolitic volcanism, thus indicating that the formation of the domes was a product of resurgence (Omenda, 1998).

Most of the faults in GOVC are buried by a thick pyroclastic cover, but vertical permeability along the N-S faults and fractures is characterised by the occurrence of the fumaroles, highly altered grounds and silica and sulphur deposits on the surface.

3. SAMPLING AND ANALYSES

3.1 Sampling

Sampling of drill cuttings from geothermal wells is crucial since the cuttings give very important subsurface information, enabling the development of geological and hydrothermal alteration models of the geothermal reservoir. In Olkaria, samples were taken at 2 m intervals and were stored in clearly labelled plastic bags but, in cases where sampling proved difficult, samples were taken at 4 m interval.

Information obtained from the cuttings is very important, particularly to the driller, as it acts as a guide, provided by the geologists, to prevent situations such as imminent eruptions (blow-outs), collapse of formations, sticking of the drill string and rapid wearing of bits. Difficulties encountered when collecting samples include delay in the time that rock cuttings take to reach the surface, especially from greater depths, but this is corrected by calculating the travelling time of the cuttings. Mixing of cuttings is another problem, whereby cuttings from shallower depth fall down, due to cave-ins while drilling, making it difficult to identify rock types.

3.2 Analytical methods

3.2.1 Binocular microscope analysis

This type of analysis is usually done during drilling to identify the formations penetrated, the fracture intensity within the formations and to identify the type and degree of hydrothermal alteration. The samples are washed and cleaned thoroughly with tap water to remove unwanted mud/clay and other contaminants encountered during the drilling operation. Then, representative samples from the washed cuttings are placed into a petri dish and mounted onto the stage of the binocular microscope. Among the essential features noted are the colour(s) of the cuttings, rock type(s), grain size, rock fabrics, original mineralogy, alteration mineralogy, and alteration intensity.

This information helps in making important decisions while drilling, such as deciding where to set the production casing, predicting loss zones, or deciding on the final drilling depth. This analysis also serves as the primary and essential base for obtaining geological data regarding the subsurface lithology, the distribution of hydrothermal minerals, and the alteration zones of the geothermal wells, allowing a gradual establishment of a conceptual model of the geothermal system.

3.2.2 Petrographic microscope analysis

The petrographic microscope is used to confirm the rock type, the hydrothermal mineral assemblages and additional minerals that were not observed under the binocular microscope. It is also used to define the mineralogical evolution encountered by studying alteration mineral sequences. This is done by selecting samples which best represent the various lithological units encountered while drilling the well. The samples are then cut and glued on glass using epoxy and polished down to a thickness of

approximately 30 μm . The analysis gives specific information, particularly on mineral types and sequences in vein and vesicle fillings.

3.2.3 X-ray diffractometer analysis

The X-ray diffractometer is mainly used in geothermal research to identify different types of clays in a given hydrothermal system. Samples are selected from the different stratigraphic units, prepared and then run for analysis of clays. Minerals are identified based on peak locations and heights in the XRD spectra. This information is important in classifying the various types of clays which, in turn, provide information on the alteration temperatures and the different alteration zones. It also helps in understanding the behaviour of the geothermal system and determining the extent of alteration.

3.2.4 Fluid inclusion analysis

This analytical method involves the analysis of fluid inclusions inside minerals by acquiring information on the temperatures at which the fluid was trapped. Fluid inclusions are small portions of fluid, which are trapped in a solid crystal as it grows or recrystallizes. The fluids are samples from the original brine from which the crystal grew, or of a much later fluid that bathed the crystal during crystallization. Primary inclusions occur as isolated inclusions distributed within the crystals, while secondary inclusions are trapped along healed cracks (Roedder, 1984). When the crystal cools, the liquid cools faster than the solid, resulting in the formation of a gas bubble. This bubble forming process can be reversed to determine the temperature at which the mineral was formed and this is referred to as the homogenisation temperature (T_h). Quartz grains were used for fluid inclusion analysis in this study to obtain the T_h temperatures.

Data obtained from all the above analyses were compiled and plotted using Log Plot (from Rockware); the software allows one to display all the geological and geotechnical data as a graphic model for easy reference and future comparison studies.

4. BOREHOLE GEOLOGY

Surface exploration was one of the first very important steps undertaken in the evaluation of the Olkaria Domes geothermal field, before any drilling was conducted. Geophysical, geochemical and geological studies were carried out producing positive results; siting of the first three initial exploratory wells was decided based on this information. Drilling of the exploratory wells gives us the vertical and horizontal extent of the geothermal reservoir, its thermal and hydrological characteristics and structures controlling the flow of geothermal fluids. Production drilling is then conducted with the aim of extracting energy from the geothermal system. Below is a description of the drilling and stratigraphy of well OW-916; this well was the 22nd well to be drilled in the Domes Field of Olkaria.

4.1 Drilling of well OW-916

Well OW-916 is one of the production wells drilled in the Olkaria high-temperature geothermal field. The well is located on the southeast side of the Olkaria Domes geothermal field (Figure 6), its coordinates being E = 204859.26 and N = 9899095.62 and the elevation 2040.83 m a.s.l.

The objective of drilling the well was to appraise the Olkaria Dome field in order to determine the major subsurface structures that control the geothermal system. Drilling was carried out by a Chinese company, Great Wall Drilling Company (GWDC), under the special supervision of Kenya Electricity Generating Company (KenGen), and was carried out in four stages, starting on 18th February, 2010 and ending on 16th April, 2010, 58 days in total, as shown in Figure 7.

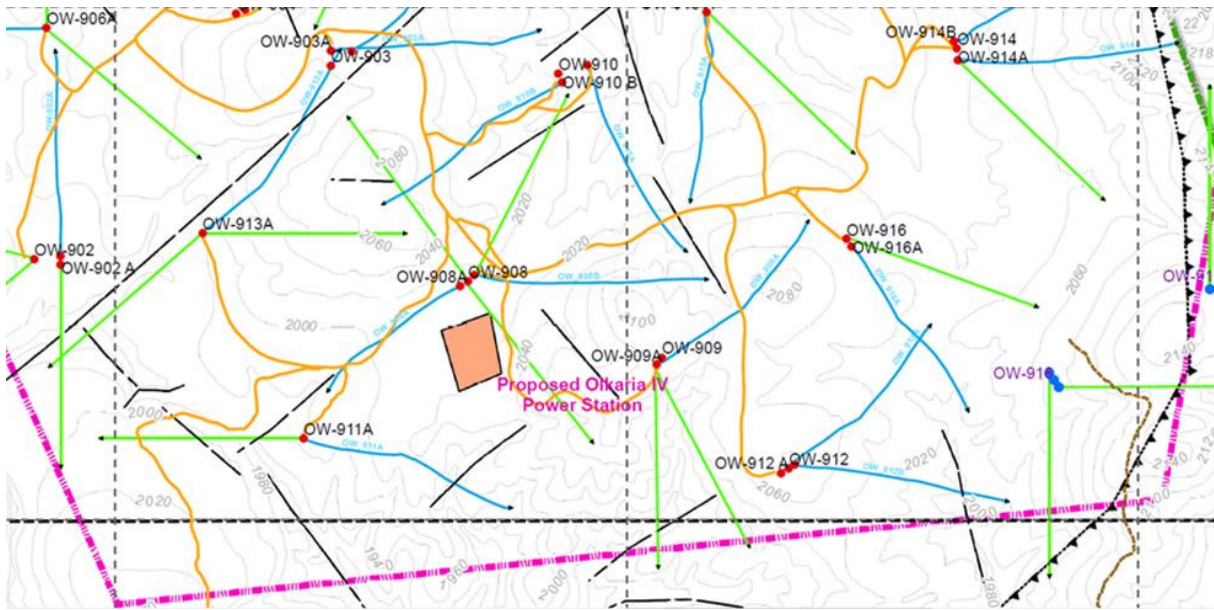


FIGURE 6: Location of well OW-916; both blue and green paths indicate direction of wells with the blue lines representing drilled wells while green lines represent wells that have not been drilled (KenGen, unpublished data)

First stage (pre-drilling): The well was spudded at 17:15 hrs. on the 18th February, 2010 with drill rig GW-188; it involved drilling with a 26" inch drill bit down to 56 m using mud, and then a 20" surface casing was installed. For the cementing job, 20.3 tonnes of cement were used.

Second stage: Involved drilling using a 17½" bit down to 308 m using water as a circulation fluid, but due to continuous loss of circulation returns from 82 m to 176 m, aerated water and foam were introduced. A 13⅜" anchor casing was installed and about 155.88 tonnes of cement were used during cementing.

Third stage: Drilled using a 12¼" bit down to 950 m using aerated water and foam with good circulation returns except between 352 and 370 m where circulation losses were experienced. A 9⅝" production casing was installed. Cementing job was done and about 59.1 tonnes of cement were utilised.

Fourth and final stage: Involved drilling using a 8½" bit down to the bottom of the well with aerated water and foam with major circulation

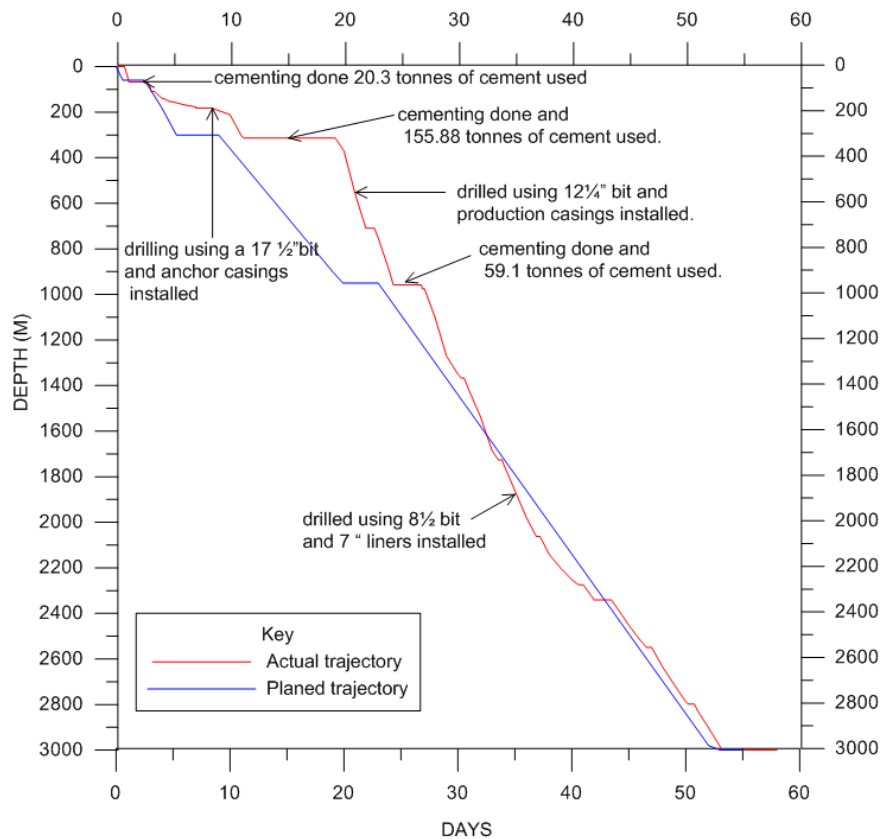


FIGURE 7: Drilling progress of well OW-916

losses experienced between 2268 and 2284 m, 2334 and 2402 m, 2542 and 2564 m. A final depth of 2994 m was reached on 12th April 2010 and a 7" slotted liner was installed. Well completion tests were then conducted for two days, showing an increase in temperature with depth; the master valve was installed, signalling the end on the 16th April, 2010. An overview of all the drilling stages and casing point details are shown in Table 1.

TABLE 1: Drilling and casing depths in well OW-916

Drill rig	Stage	Depth (m)		Casing type	
		From	To	Width (")	Type
GW-188	Pre drilling	0	56	20	Surface casing
GW-188	1st stage	56	308	13 ³ / ₈	Anchor casing
GW-188	2nd stage	308	950	9 ⁵ / ₈	Production casing
GW-188	3rd stage	950	2994	7	Slotted liners

4.2 Stratigraphy of OW-916

The types of rock that were encountered in this well were pyroclastics and tuffs dominating the upper 500 m, while below 500 m lava rocks, together with tuffaceous intercalations, dominated. Porosity is quite high in tuffs while rhyolites and trachytes have their porosity and permeability controlled by fractures. The rate of penetration (ROP) during drilling reduced significantly below 2300 m, as did the alteration. Minor intrusions were encountered but trachytes and rhyolites were most abundant by volume with a few basaltic lavas being found. High alteration was observed between 600 and 1500 m with intense vein and vesicle filling at these depths. Petrographically, the rocks are similar to those encountered in other wells drilled in the Olkaria geothermal field. Classification of the different lava types was based on the texture, colour, alteration and constituent minerals present. The data is presented with help of LogPlot from Rockware (2007).

The following description of the rock formation is based on binocular observations, aided by petrographic thin sections and XRD analysis. A detailed description of the cuttings is comprehensively given in Appendix I.

Pyroclastics. These form the uppermost 82 m of the well (Figure 8). They are brown to grey in colour, unconsolidated, unaltered and contain a mixture of pumice, obsidian and other rock fragments with euhedral crystals of quartz and feldspars (sanidine). Slight oxidation is exhibited in some of the rock cuttings. Low-temperature zeolites are also found in this formation.

Tuffs are spread throughout the well, intercalating with other formations or as thick layers, varying in thickness from 6 up to 100 m. The dominant tuff deposits are between 368 and 636 m. The tuffs occur in different forms and four varieties were observed:

Crystalline tuff, which is brown in colour and contains a high percentage of quartz phenocrysts in its groundmass; it was observed between 266 and 306 m.

Vitric tuff, which is heterogeneous, glassy and brown to light brown in colour, contains smaller amounts of quartz in the groundmass with secondary quartz growing in the vesicles.

Lithic tuff, had a range of different colours with the extent of alteration and oxidization depending on the composition and depth of the rock. It is mainly made up of lithics of different rock types, i.e. rhyolites, trachytes and basalts cemented in a very fine grained matrix with calcite replacing the feldspars and filling veins. Large deposits of lithic tuff were observed between 402 m and 636 m. The primary minerals are much altered and oxidised, imparting green and brown colours. Epidote

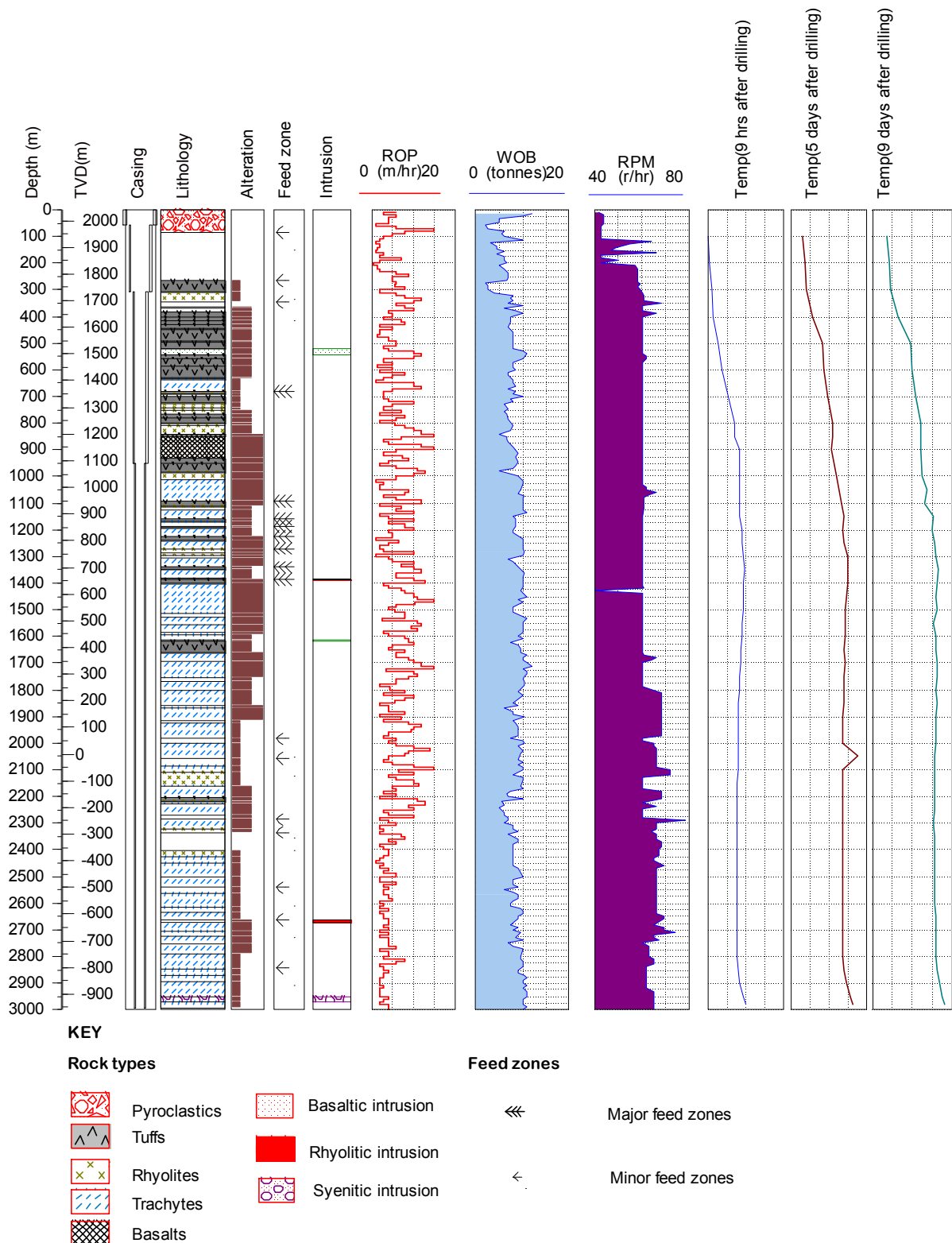


FIGURE 8: Lithology of well OW-916

was observed filling vesicles in this unit at 556 m depth. Zoning of chlorite and quartz was also observed occurring in a sequence, chlorite being deposited first and then followed by quartz.

Welded tuff shows flow banding textures and contains lithics of heterogeneous rock fragments; it was observed between 544 and 560 m, 702 and 724 m, and 1340 and 1348 m.

Rhyolites are brown, white and light grey in colour and occur intercalating with tuff formations between 306 and 1014 m, while at depths below 1110 m, they intercalate with trachytes. The upper rhyolites between 306 and 1014 m are porphyritic with abundant quartz and sanidine phenocrysts; also present are small phenocrysts of pyroxenes and magnetite. They have a spherulitic texture with some zones showing flow banding and alteration to clays. The deeper rhyolites below 1110 m occur intercalated with trachytes and tuffs; they are felsic, fine to medium grained, have low phenocryst content and lack the spherulitic texture.

Trachytes are less abundant at shallower depths and are first penetrated at 636 m, but become dominant from 1014 m to the bottom of the well, where they form thick formations with 8-20 m intercalations of tuffs and rhyolites. They are succeeded by an 82 m sequence of basaltic lava at 932 m depth. They are brown to grey in colour, fine grained to porphyritic with sanidine phenocrysts showing Carlsbad twinning in a feldspar-rich groundmass, exhibiting the flow structure characteristic of trachytes. Pyroxenes (aegerine-augite), amphiboles (riebeckite) and opaques are the other primary minerals observed in this unit. Alteration varies at various depths (see Figure 8) with high alteration between 1014 and 1984 m, with sanidine becoming completely altered to albite at these depths; alteration is less below 2002 m. Calcite and pyrite are scarce in this unit, but epidote, wollastonite and actinolite are the most common alteration minerals replacing feldspars, with epidote most commonly filling veins.

Basalts. At a depth of 526 m, a 24 m thin layer of basalt is penetrated. It is dark grey and porphyritic with plagioclase and pyroxene phenocrysts and is highly altered with abundant calcite filling veins. The other basaltic lava noted was penetrated at 850 m. It is a thick layer, about 82 m from 850 to 932 m, grey to dark grey porphyritic with pyroxene phenocrysts set in a groundmass rich in very small plagioclase laths. Olivine in this unit has been completely altered to calcite and clays, vesicles are rare but a sequence of clays, epidote and wollastonite, was observed in some vesicles and veins.

Syenitic intrusion. This intrusive is felsic, light in colour and coarse grained with large pyroxenes distributed in the groundmass. It was penetrated between 2952 and 2968 m depth and is 16 m thick, showing less alteration to clays and with some alkali feldspars as large as 4 mm in length. This intrusion forms a minor aquifer in this part of the well.

Basaltic intrusion is penetrated at 520-544 m and 1614-1618 m depth. It is dark grey, very fine grained with almost no alteration observed. Chilled glassy margins are observed on the edges of the dyke with increased alteration observed in the host rocks. Intensive silicification is also observed.

5. HYDROTHERMAL ALTERATION

Hydrothermal alteration is a general term which embraces the mineralogical, textural and chemical response of rocks to a changing thermal and chemical environment in the presence of hot water, steam or gas (Henley and Ellis, 1983). As a result of this water-rock interaction, the primary minerals which constitute the rocks are altered into different secondary minerals, and the alteration process, together with the resulting type of alteration minerals, are dependent on the type of primary mineral altered. Factors that influence the types of mineral assemblages and the distribution of hydrothermal alteration products include permeability, temperature, fluid composition (pH value, gas concentration, magmatic, meteoric), initial composition of the rocks, duration of activity (immature, mature), pressure and hydrology (Reyes, 2000).

Understanding of the hydrothermal alteration in all geothermal fields is crucial, since the data collected can give a general picture of the geothermal system in a given area and its geological history. These hydrothermal minerals can also be used during drilling to determine the depth of the production casing, estimate fluid pH, as well as predict scaling and corrosion tendencies of fluids, measure permeability, identify possible cold water influxes and act as a guide to the hydrology of the area (Reyes, 1990).

5.1 Alteration of primary minerals

Trachytes and rhyolites were the predominant rock types in well OW- 916, and the primary rock-forming minerals in these rocks include volcanic glass, olivine, feldspars, pyroxenes and opaques. Their order of alteration depends on the Bowen's reaction series where the first mineral to be formed is also the first to be altered (Figure 9). Volcanic glass, which is a constituent of these rocks, cannot be classified as a mineral, but is relevant in this discussion as its replacement products are very important hydrothermal minerals.

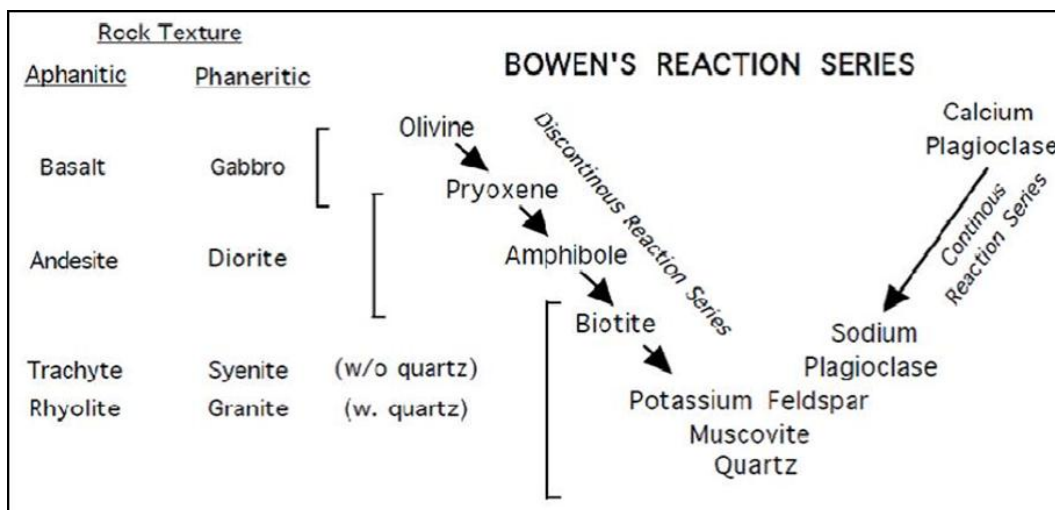


FIGURE 9: Bowen’s reaction series (from Thomas, 2010)

The primary rock minerals range from fine to coarse grained crystals. From 266 m, clays and calcite are the most common replacements of the primary minerals, together with quartz and albite from 346 m depth. The primary minerals that are mostly altered in this well are olivine, sanidine and pyroxenes, while quartz remains relatively unaltered. In the basaltic rocks, olivine and glass have been replaced by calcite and clays, while the pyroxenes and feldspars are partially altered. In trachytes, it was seen that sanidine phenocrysts showed stronger alteration to albite and clays than the sanidine groundmass.

In general, the order of decreasing susceptibility to alteration is glass, olivine, pyroxenes, plagioclase/sanidine and opaques, thus agreeing with the sequence observed in the Olkaria East field (Browne 1984). The primary minerals and their alteration products are summarised in Table 2.

TABLE 2: Primary minerals and their alteration products

Primary minerals	Alteration products
Volcanic glass	Clays, calcite, quartz, zeolites
Olivine	Clays, calcite, chlorite, actinolite
Plagioclase	Calcite, clays, quartz, epidote, albite, wairakite
Sanidine	Albite, adularia, clays
Pyroxenes	Clays, actinolite, chlorite
Opaques	Pyrite, haematite

Glass is the very first primary phase that undergoes hydrothermal alteration in this well altering to clays and also the first to be replaced, mainly by calcite and zeolites from 266 m depth. Volcanic glass was common in scoria and the different tuff formations penetrated, where it ranged from being nearly fresh to highly altered. In petrographic analysis, it appears transparent and isotropic when fresh and then brown and anisotropic due to alteration to clays.

Olivine is the least abundant and rarest primary mineral observed, due to its susceptibility to alteration, being completely altered to clays and calcite. It is very scarce or not present in trachytes and rhyolites.

Plagioclase is a primary mineral observed in basalts with a similar appearance as quartz, except that it has cleavage, is milky in colour and forms characteristic brown alteration products. It occurs as fine grained groundmass in rocks that exhibit porphyritic texture. Under the petrographic microscope it is readily identified by its low relief and polysynthetic twinning. It is relatively unaltered at shallower depths but becomes progressively altered with depth to clays, calcite, epidote and albite.

Sanidine is common in trachytes from 636 m depth, showing alteration to albite and clays. It is colourless in thin sections and clouding is sometimes common; it has low relief, low birefringence and Carlsbad twinning is clearly observed. Cleavage is sometimes not visible in thin sections due to low relief. Quartz is similar to sanidine but is uni-axial.

Pyroxene is most abundant in the basaltic formations in this well, where it occurs as clinopyroxene phenocrysts in a plagioclase-rich groundmass, and in the syenitic intrusion, where it is coarse grained. In trachytes, aegerine-augite is observed. It appears dark and shiny with a metallic lustre and is identified in thin sections by its good cleavage and inclined extinction. Generally pyroxenes are resistant to alteration in this well, but become progressively altered to actinolite and clays from 1030 m down to the bottom of the well.

Opaques appear dark and show a high resistance to alteration and comprise mainly FeTi-oxides, but they are generally crystallised as part of the primary rock constituents. However, in places, especially near the intrusive margins, opaque minerals, e.g. magnetite, form as a part of the contact aureole.

5.2 Distribution of hydrothermal alteration minerals

The hydrothermal mineral assemblages found in this well are similar to those found in other high-temperature fields around the world (Browne, 1978). Below is a description of the hydrothermal alteration minerals encountered in well OW-916. Their distribution is shown in Figure 10.

Chabasite: Low-temperature zeolite stable between 30 and 80°C; was only observed at 52 m. It was milky white, had a tabular/cubic structure and was observed in a vesicle.

Wairakite: High-temperature zeolite stable at temperatures above 200°C. It was only observed in thin sections and occurs rarely. According to Figure 10, it occurs between 300 and 600 m. It is colourless with low relief in plane polarised light, while with crossed polars it exhibits perpendicular polysynthetic sets of twin lamellae, which are similar to microcline, but wairakite exhibits poor cleavage.

Chalcedony: Low-temperature mineral which was observed intermittently in this well in vesicles and veins, mostly in the upper 400 m, but in most cases it was altered or replaced by quartz, because it is very unstable at temperatures higher than 180°C.

Pyrite was observed from 266 m and was seen to be abundant in the upper tuff formation, but became rare from 850 m to the bottom of the well. It occurs as euhedral cubic crystals with brassy yellow lustre in reflected light. Cubic crystals of pyrite were observed as disseminations in the groundmass or as deposits in fractures, veins and vesicles. Pyrite is one of the alteration minerals that indicate good permeability in a formation.

Calcite: This mineral is usually aggressive as a replacement mineral, and in this well it was first noted from 266 m, replacing feldspars (plagioclase and pyroxenes) and volcanic glass. It also filled veins and vesicles but rarely appeared as platy calcite. Under the binocular microscope, it was white to colourless and was identified by testing it with dilute hydrochloric acid; in thin sections it was identified by its high

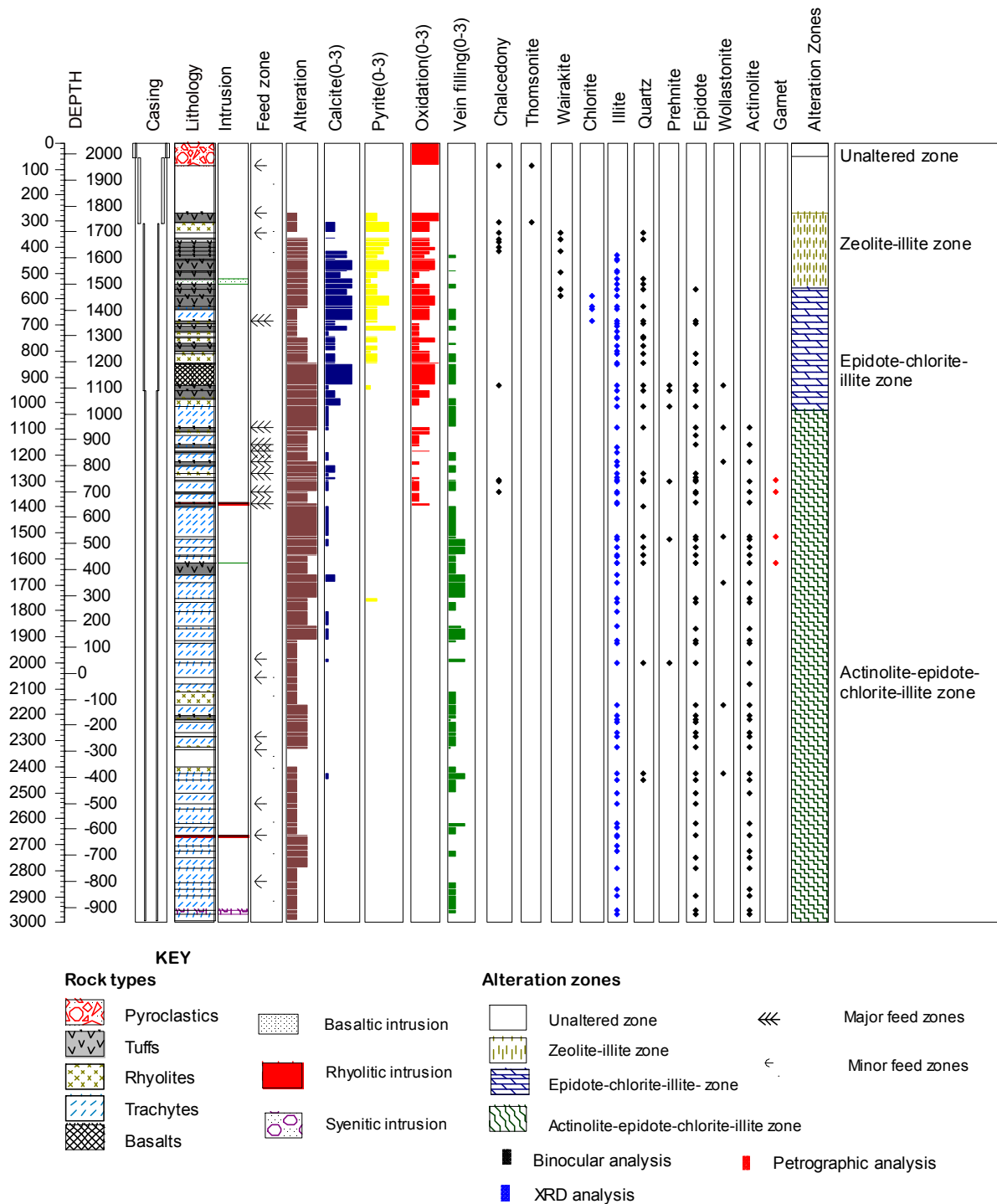


FIGURE 10: Hydrothermal alteration minerals in well OW-916

birefringence and pronounced change in relief when the stage was rotated. Disappearance of calcite was noticed below 1900 m depth and this can be attributed to the high temperatures (>300°C) where it becomes unstable.

Quartz is colourless and exhibits a clear prismatic shape and was seen growing in vesicles and veins together with epidote, prehnite and calcite as a secondary mineral from 300 m to the bottom of the well, indicating temperatures above 180°C. Under the petrographic microscope, it has undulating extinction, low relief, low birefringence and no clear twinning. This is used to differentiate it from feldspars and

zeolites. Secondary quartz does not show subsequent alteration, since it is stable even at high temperatures.

Albite is milky white (cloudy) in appearance, has a euhedral shape and was often observed replacing primary minerals, K- feldspars (sanidine) and plagioclase feldspars, a process referred to as albitization, indicating temperatures above 180°C. It was observed from 440 m to the bottom of the well. In thin sections, it has a cloudy appearance, low refractive index and its formation involves the destruction of the characteristic plagioclase feldspar twinning habit.

Prehnite is a high-grade alteration mineral formed at temperatures above 240°C occurring sporadically in the well from 860 to 2000 m depth. It was observed under the binocular microscope as a vein and vesicle filling mineral in association with epidote, quartz, wollastonite, albite and clays, exhibiting a box-like cleavage. In thin sections, it has strong birefringence, good cleavage in one direction and a characteristic sheaf-like (bow-tie) structure.

Epidote was first observed at 556 m as yellowish green, radiating, prismatic crystals growing in a vesicle, indicating temperatures of over 240°C at this depth. It mainly occurred as a vein filling and vesicle filling mineral and in some cases replacing plagioclase, sanidine and pyroxenes. Under the petrographic microscope, it was identified as having high relief, a green to light yellow colour and exhibiting pleochroism, but the colour of epidote can be attributed to varying amounts of iron in the mineral. The first appearance of epidote indicates that the well has entered the geothermal reservoir and thereby aids in determining at which depth the production casing should be set.

Wollastonite is white in appearance, exhibiting a hairy, radiating, compact and fibrous structure, and was first observed filling vesicles at 914 m together with epidote, and occurs intermittently to 2400 m depth. It is colourless with low birefringence in thin sections and its occurrence indicates temperatures of 270°C and above.

Actinolite is a high-temperature mineral that is formed at temperatures above 280-290°C and was observed from 1030 m to the bottom of the well, replacing pyroxenes and filling vesicles. It is pale green to white in appearance, occurring as thin colourless and elongated crystal laths or as radiating and fibrous crystal aggregates. In thin sections, it has moderate pleochroism with moderate relief.

Garnet was only observed in thin sections from 1290 to 1600 m depth in a sequence of trachytes intersected by a dyke and tuffs. Clusters of euhedral, brown crystals were observed in plane polarised light, while in crossed polars it was isotropic, a characteristic of garnets. The presence of garnet usually indicates temperatures above 290-300°C.

Clays are the most common and dominant hydrothermal alteration minerals that are observed in this well. These are water-rich phyllosilicates that are formed by alteration of primary silicate minerals and require the presence of water in liquid or vapour form (Njue, 2010). They are finely crystalline or meta-colloidal and occur as flake-like or dense aggregates of varying types (Pendon, 2006). The primary rock forming minerals in this case are altered to different types of clays, depending on the temperature, fluid composition, pH and the permeability of the formation. Plagioclase and pyroxenes are rather resistant to alteration, but volcanic glass is very unstable and is usually easily altered to clays. The clays in this well form in veins, vesicles or as replacements and are fine to coarse grained in texture.

Four types of clays were identified from the surface to the bottom of the well, based on binocular analysis, petrographic analysis and XRD analysis, and a brief description is given below; their results are shown in Appendix II.

Smectite was observed in small quantities in this well. Smectite is brown to green, fine grained and under the microscope it is observed replacing primary minerals or filling veins and vesicles. It forms at temperatures below 200°C (Franzson, 2011). XRD analysis shows the swelling nature

of smectite clays, with peaks indicating layer spacings in untreated samples of 13.05-15.47 Å, peaks of 13.64-17.53 Å in glycolated samples, but small spacings are seen when smectite is heated with peaks between 7.76 and 10.14 Å.

Mixed-layer clays are intermediate products of pure end member clays and are fine to coarse grained, as observed from the binocular microscope, and were identified intermittently between 700 and 1200 m in this well. In thin sections, they are mostly brown to green with strong pleochroism with plane polarised light. In XRD analysis, they show characteristics that are similar to chlorite and illite, with peaks of 12 Å in the untreated, glycolated and heated samples, respectively.

Chlorite was first observed from 578 to 680 m, showing a wide range of different textures, forms and colours; its appearance indicates temperatures above 200°C but it can also be stable above this temperature. Chlorite is fine to coarse grained, has low birefringence and is dark to light green under the petrographic microscope, but exhibits anomalous interference colours (blue, purple, brown). Its texture shows tiny green needles, occurring sometimes as radial forms in veins and vesicles, in association with prehnite, epidote, wollastonite, calcite and quartz, but also in some cases replacing feldspars. XRD analyses of chlorite show both the stable and unstable types. Stable chlorite has consistent peaks of 7.0-7.2 Å, and peaks of 14.0-14.5 Å in the untreated, glycolated and heated samples, respectively; unstable chlorite shows similar peaks, but the peak at 7.0-7.2 Å disappears (collapses) when the sample is heated.

Illite was observed from 418 m to the bottom of the well and is the most common clay observed in this well. It is light green to white in colour, occurring in veins, vesicles and replacing K-feldspars. XRD analyses show a persistent peak of 10 Å in untreated, glycolated and heated samples. It indicates temperatures of 200°C and above.

5.3 Vesicle and vein fillings

Vesicles and veins are the main hosts for hydrothermal alteration products, and they usually dictate the porosity and permeability of a well. Vesicles are pore spaces filled by the deposition of secondary minerals or by fluid, while veins are small fractures in rocks filled by secondary minerals or fluid. Their identification, which is achieved by the binocular and petrographic microscopes, is critical since alteration mineral sequences in the vesicles show temperature conditions and changes that have occurred throughout the lifetime of the geothermal reservoir. Vesicles are more abundant in the tuff formations and are less abundant in trachytes, rhyolites and basalts. Vein fillings are less abundant in the tuff formations but become abundant in the fractured trachytes, basalts and rhyolites from 850 m depth to the bottom of the well.

In well OW-916, the upper rock formations, above 550 m, show vesicles filled with quartz and clays, but moving deeper below 550 m, epidote was observed growing in a vesicle with a vein filling of clays and calcite, indicating a rise in formation temperature to accommodate the formation of epidote. Below 900 m, vesicle and vein fillings of epidote, prehnite, wollastonite and actinolite were observed, indicating an increase in temperature with depth.

Vein fillings are abundant in fractured rhyolites, basalts and trachytes between 650 and 2000 m and this correlates with the areas where major feed zones in this well are located.

5.4 Sequence of mineral deposition and paragenesis

The sequence of mineral deposition in a geothermal system is very important when studying the evolution of the field over time, while at the same time predicting the future if all parameters are kept

constant (Brown, 1984). In determining the evolution of the geothermal system, the mode of occurrence of the alteration minerals is critical and also their dependence on temperature, chemistry of the fluids, rock type, the interaction between the hydrothermal fluids and the host rock, porosity, permeability and the duration of the interactions (Reyes, 2000). This is revealed by studying the hydrothermal minerals deposited in veins and vesicles and subsequently both the gradual progression of mineral deposition over time and their sequence is established (Muchemi, 1985).

Vein fillings in this well were abundant from 650 to 2000 m, with depths above 500 m having mineral sequence depositions mainly confined to vesicles whereby fine grained clays were deposited first, followed by a coarse grained layer of mixed-layer clay, with quartz occurring last. This indicates a rise in temperature from the precipitation of low-temperature fine grained clays to the formation of quartz.

In depths below 900 m, vein fillings and vesicles mostly showed three zones of deposition, fine grained clay being deposited first, followed by epidote, with wollastonite or actinolite forming last, indicating the geothermal system was evolving from low-temperature conditions to high-temperature conditions (Figure 11).

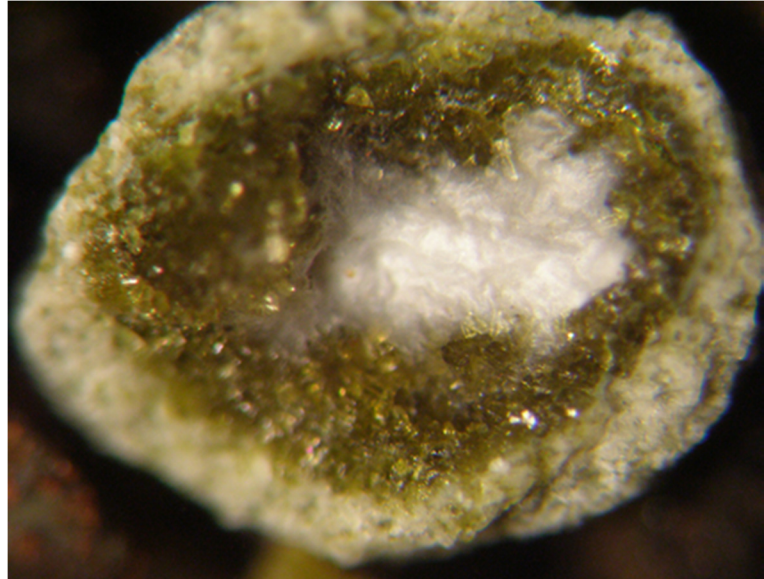


FIGURE 11: Mineral sequence deposition at 914 m depth showing epidote forming first followed by wollastonite

5.5 Mineral alteration zones

Alteration mineralogy is very important in determining the hydrothermal conditions present in the well or the geothermal reservoir and can also be used to reflect past temperatures that have existed over a given period of time (Agonga, 1992). The mineral alteration zones in this well were built on the basis of binocular and petrographic analyses to identify the different hydrothermal alteration minerals, and XRD analyses to obtain the clay mineralogy data. The minerals most commonly used for prediction of temperatures in this well are epidote, prehnite, wollastonite, actinolite and clays. The alteration zones are characterised by the abundance of particular minerals and clays, which are related to increasing temperature with depth. These zones can be used to produce isotherms to compare with the measured temperatures of the well.

Based on the hydrothermal alteration mineral assemblages in Olkaria Domes geothermal field, three different zones of alteration can be recognised. The boundary from one zone to the other was defined by the first appearance of the successive dominant alteration mineral, while the upper 50 m of the well is relatively unaltered. No cuttings were retrieved in the interval 84-266 m. The zones are:

Unaltered zone (0-84 m): This zone is characterised by pyroclastic rocks showing high levels of oxidation which is not related to geothermal activity. Few alteration minerals are observed, but alteration is due to interaction of the rocks with cold groundwater. XRD analyses show no clays in this zone.

Zeolite-illite zone (266-556 m): This zone is characterised by the first appearance of zeolites at 266 m depth. Zeolites are scarce in this well, occurring between 266 and 556 m (Figure 10). Illite, a high-temperature clay indicating temperatures above 200°C is also found in this zone. Illite, identified through XRD analyses, is fine grained and white to light green in colour. It occurs as a replacement of K-feldspars and pyroxenes and as vein and vesicle fillings, together with calcite and pyrite. In this zone, feldspars are also altered to albite; other hydrothermal minerals observed include smectite and mixed-layer clays, which are coarse grained.

Epidote-chlorite-illite zone (556-1030 m): This zone is characterised by the first appearance of epidote at 556 m depth, indicating temperatures of over 240°C. Alteration is intense and mineral assemblages observed in this zone include prehnite, wairakite, quartz, calcite and pyrite and wollastonite. Chlorite and illite clays are seen replacing feldspars and filling veins and vesicles. XRD analyses indicate that unstable chlorite is present, but the co-relationship between lithology and the type of chlorite clay, which forms (whether stable or unstable), is still not understood. A high percentage of the primary minerals completely altered indicates intense hydrothermal activity in this zone. Oxidation is also relatively high.

Actinolite-epidote-chlorite-illite zone (1030-3000 m): This zone is characterised by the appearance of actinolite at 1030 m depth, extending to the bottom of the well. Garnet in this zone appears rarely and is only observed by thin section analysis from 1290 m, occurring sporadically between 1290 and 1650 m (Figure 10). Actinolite and garnet indicate temperatures over 290-300°C. Actinolite is observed replacing pyroxenes from 1030 m depth and, in some cases, filling veins.

5.6 Aquifers

Drilling in a prospective geothermal field is proven successful if high-temperature permeable zones are intercepted. The permeable zones (aquifers) are either cold or hot and are defined by faults, fractures, lithological contacts and intrusions intercepted while drilling. These zones are also identified by geophysical logs, and the hydrothermal alteration and loss of circulation zones encountered. Drilling parameters such as the pumping rate, rate of penetration and weight on the bit are also used in locating probable aquifers. Cold aquifers encountered in the upper parts of the well are cased off and carefully cemented to prevent them from interfering with the production of the well.

Permeability zones identified in the Olkaria Domes geothermal field are dependent on fractures due to intrusions and along the edges of plugs and domes. They also occur in contact zones between formations and highly fractured and fragmented contacts in some formations (Lagat, 2004). Temperature logs during and after drilling, circulation loss zones, lithological contacts and hydrothermal alteration were the main parameters that were used in locating aquifers in OW-916. An abundance of pyrite and calcite observed during drilling also indicate zones of permeability. Alteration intensity in this well has a close relationship with the permeable zones intersected, with areas experiencing high alteration indicating high permeability, while areas of low alteration correlate with areas of low permeability.

Permeable zones identified from the temperature logs correlate with geological observations that were made. Minor circulation losses could not be identified, since circulating fluid coming from the well during drilling was not measured and, thus, small aquifers were not identified.

Data obtained from temperature logs, hydrothermal alteration and circulation losses (Figure 12) show the locations of aquifers encountered in this well. Major feed zones were located between 650 and 1400 m and are associated with fractured trachyte formations, rhyolitic intrusion and lithological contacts between the different trachytic formations and minor tuffs, as shown in Table 3.

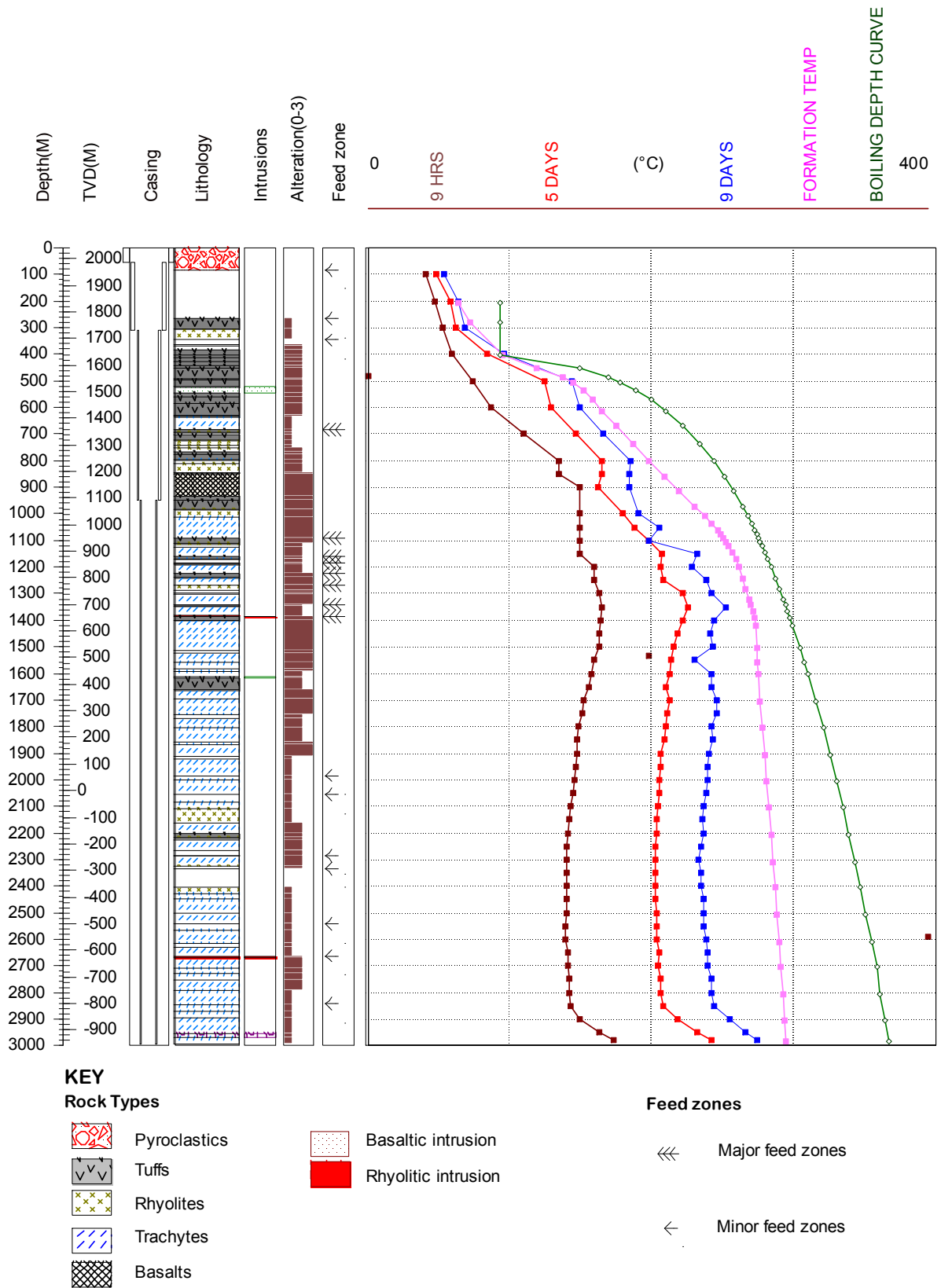


FIGURE 12: Feed zones in well OW-916 and temperature logs subsequent to drilling. Formation temperature and boiling depth curve are shown in purple and green respectively

TABLE 3: Interpreted permeable zones\ aquifers based on geological observations

Depth (m)	Evidence from geological observations and drilling observations
84-266	Circulation losses
266-306	Associated with primary permeability in tuff
344-364	Fractured permeability in rhyolite
682-692	Associated with primary permeability in tuff
1160-1168	Contact between trachyte and tuff
1224-1240	Contact between fractured trachyte and tuff
1270-1270	Associated with rhyolitic intrusion
1330-1340	Contact between fractured trachyte and tuff
1386-1400	Associated with primary permeability in tuff
1984-2002	Circulation losses
2056-2084	Circulation losses
2286-2290	Contact between rhyolite and trachyte
2334-2402	Circulation losses
2662-2670	Fractured trachyte
2842-2848	Fractured trachyte

6. FLUID INCLUSION GEOTHERMOMETRY

This is a method whereby inclusions trapped in minerals during crystallisation or recrystallization are analysed to determine the temperature at which the vapour that they contain disappears; this refers to the temperature at which the fluid \pm gas became trapped in the crystal, and it is referred to as the homogenisation temperature (T_h). Fluid inclusions provide vital information concerning the history of a geothermal field and can be used to determine the thermal history of the system.

Quartz crystals were used for the analysis of fluid inclusions in this well and the homogenisation temperatures were recorded. The homogenisation values at 1600 m depth ranged from 275 to 305°C and the estimated formation temperature at this depth is 276°C.

Thirteen fluid inclusions were studied and a histogram was then drawn showing the temperatures at which different inclusions homogenised (Figure 13). The relationship between measured temperatures, hydrothermal alteration temperatures, the boiling depth curve and fluid inclusion temperatures was studied to understand how the geothermal system has evolved with time, shown in Figure 14.

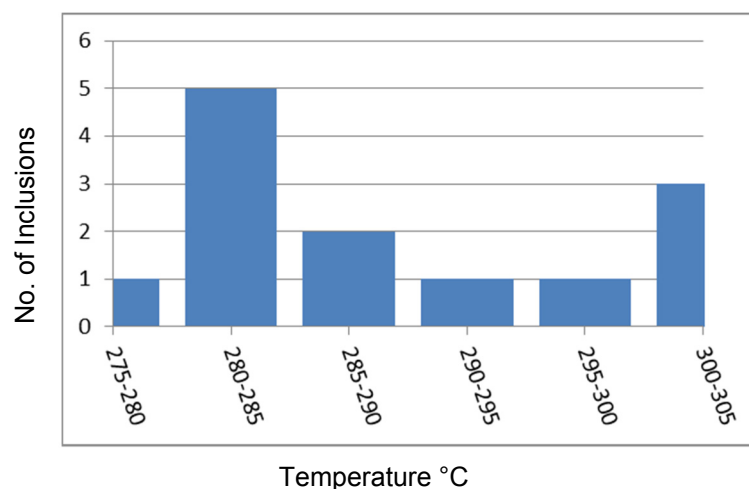


FIGURE 13: Histogram showing the results of fluid inclusion analyses in OW-916

The relationship between the four parameters shows that the geothermal system has cooled $\sim 25^\circ\text{C}$, when comparing the estimated formation temperature with the first appearance of selected hydrothermal alteration minerals. For example, epidote was first observed where the measured formation temperature was below its

temperature stability range, indicating that it was formed under the past geothermal conditions that prevailed in this system.

But fluid inclusion temperatures seem to reflect current conditions; the average homogenisation temperature of 282°C is close to the measured formation temperature of 276°C, indicating quartz crystals recrystallized within this temperature range. This indicates that the system is in a state of equilibrium.

7. DISCUSSION

Generally, the geology and rock types encountered in this well are similar to that of other wells in the Olkaria Geothermal field (Lagat, 2004). The stratigraphy of the upper 3000 m consists of tuffs, rhyolites, trachytes, basalts and intrusions. Trachytes are the dominant lava rocks in this field and are more voluminous than the other lava rocks observed. Rocks observed in this well show extensive alteration and water-rock interaction below 266 m depth, and were divided into different units based on rock composition, textural differences and the intensity of alteration.

Four different types of tuffs were identified and show extensive alteration with the major tuff deposits being found between 368 and 636 m. Two types of rhyolites were observed; the upper rhyolites between 306 and 1014 m are porphyritic with quartz and sanidine feldspars in a felsic groundmass, while the lower rhyolites, below 1110 m, are less porphyritic and show an abundance of pyroxenes. Trachytes were also divided into two types: the trachytes between 636 and 1190 m which are porphyritic, intercalated with tuffs, rhyolites and basalts, and the trachytes below 1190 m which are less porphyritic. They show high alteration in the contact zones between trachytes and tuffs, brecciated areas and areas where fractures and veins are intense. Riebeckite and aegerine-augite are characteristic minerals in these rocks.

Illite is the most abundant clay mineral in this well, occurring in vesicles, veins and replacing feldspars. The hydrothermal mineral assemblage is similar to that found in other wells in the Olkaria geothermal field, consisting of prehnite, epidote, wollastonite, actinolite, garnet, quartz and zeolites, and they are mainly present in vesicles, veins and as replacements of primary minerals in volcanic rocks.

On the basis of hydrothermal alteration minerals and their variations with depth, three hydrothermal mineral zones can be recognised in order of increasing temperature and depth. They are the: (1) zeolite-illite zone, (2) chlorite-illite-epidote zone, and (3) actinolite-epidote-chlorite-illite zone, while the uppermost 50 m is relatively unaltered. Hydrothermal deposition sequences in veins and vesicles

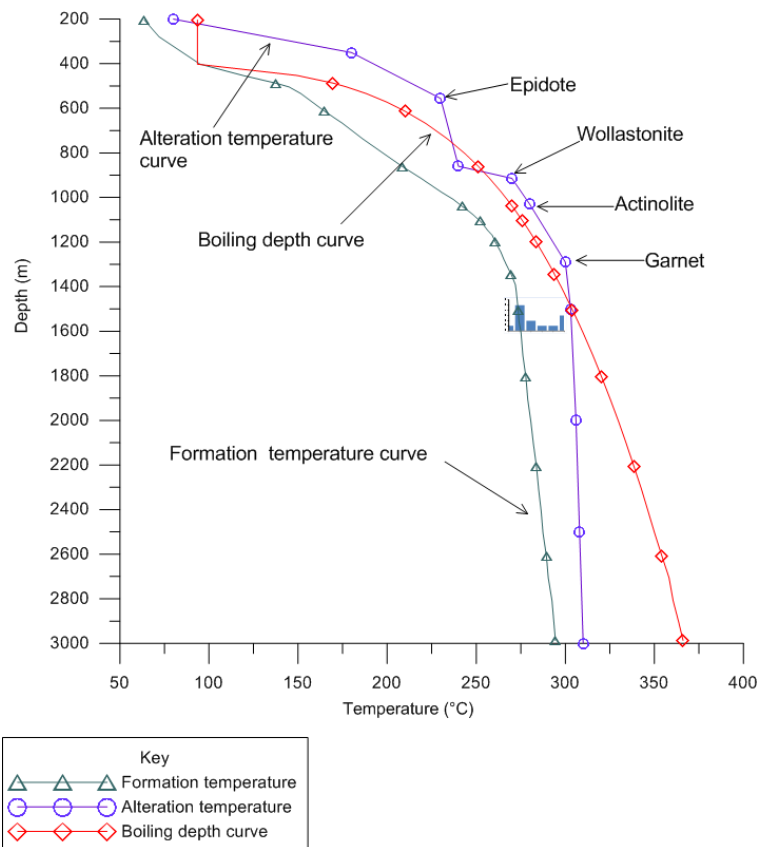


FIGURE 14: Relationship between fluid inclusions (T_h), formation temperature, alteration temperature and the boiling depth curve of OW-916

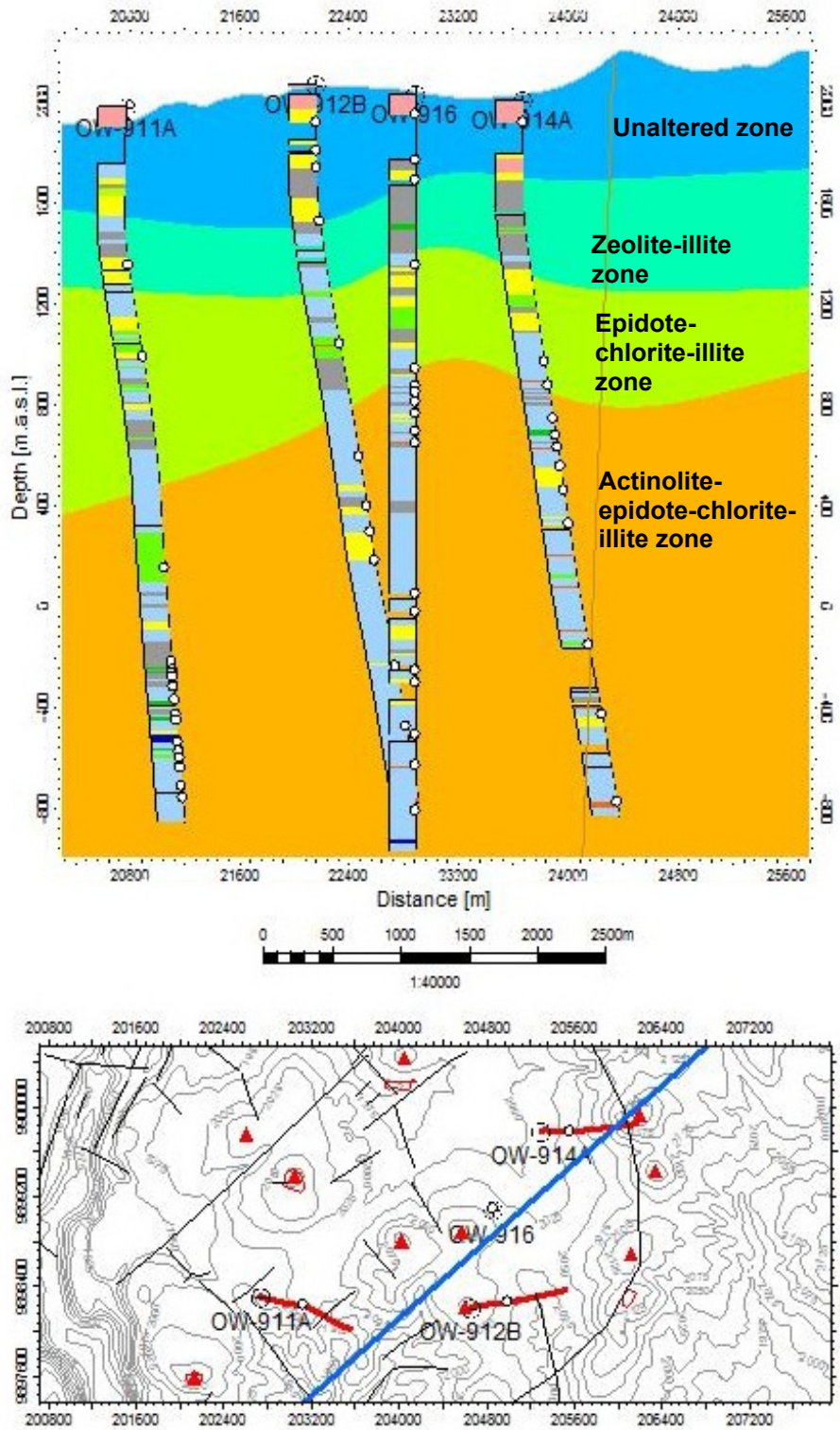


FIGURE 15: A cross-section of wells OW-911A, OW-912 B, OW-916 and OW-914A; the zone to the northeast has been extrapolated

occurring in this well imply that the system has consistently been heating up with time. Comparison between wells OW-916, OW-914 A, OW-912B and OW-911 A in the Olkaria Domes geothermal field shows rocks that have similar alteration at different depths (Figure 15); in well OW-916 high alteration minerals, epidote and actinolite, are found at a shallower depth when compared to the other wells, well OW-912 B, OW-911 A and OW-914 A, indicating the site of a possible up flow zone.

Binocular analyses indicate the presence of actinolite at 1030 m, while the measured formation temperature is lower than the stability range for the formation of actinolite, showing that the temperature of the system was higher in the past, indicating that the geothermal system has cooled since the peak of hydrothermal alteration.

A study of fluid inclusions in quartz shows homogenisation temperatures ranging from 275 to 305°C, but with an average temperature of 282°C, which is close to the measured formation temperature of about 276°C. This indicates that the inclusions formed at thermal conditions similar to the present ones in the reservoir. This may imply that the system at this location is actually in a state of equilibrium.

Feed zones in this well which were intercepted are associated with fractured trachyte and rhyolite formations, rhyolitic intrusion and lithological contacts between the different trachytic formations and minor tuffs. Major feed zones are between 650 and 1400 m. A comparison between four wells in Olkaria Domes geothermal field, i.e. wells OW-916, OW-914 A, OW-912B and OW-911 A, shows that the major feed zones in this field are between 600 and 1600 m (Figure 15) and are tied to lithological contacts, fractured rock formations and intrusions.

8. CONCLUSIONS

- The lithology of well OW-916 is composed of pyroclastics, tuffs, rhyolites, basalts, trachytes and minor basaltic and rhyolitic intrusions, showing similar stratigraphy with the other wells drilled in this field.
- Hydrothermal alteration minerals in this field are controlled by temperature, permeability and rock types.
- Three alteration zones were identified, based on hydrothermal mineral assemblages, and include: (1) zeolite-illite zone, (2) epidote-chlorite-illite zone, (3) actinolite-epidote-chlorite-illite zone; the uppermost 50 metres are relatively unaltered.
- Binocular and petrographic analyses of mineral sequences in vesicles and veins show a gradation of hydrothermal alteration minerals from low-temperature to high-temperature, indicating a history of heating in the geothermal system. Slight cooling seems to have occurred when comparing the formation and alteration temperatures.
- Measurements and studies of fluid inclusions in this well and a comparison with neighbouring wells show that the system may be in a state of equilibrium. However, alteration temperature logs indicate that temperatures were higher in the past.
- Aquifers in this well show close association with fractured formations, lithological contacts between formations and, in some cases, intrusions at depth.
- In this well, high permeability correlates with high alteration between 650 and 1400 m, fracturing and vein and vesicle fillings at these depths.
- High permeability in this field is indicated by the high abundance of pyrite and calcite, high alteration intensity, fracturing and high occurrence of veins, while low permeability is identified by low alteration and the absence of key alteration minerals.

ACKNOWLEDGEMENTS

My utmost appreciation and gratitude go to: UNU-GTP for giving me the chance to come to Reykjavík, Iceland and undertake this course; to Dr. Ingvar Birgir Fridleifsson, Director of UNU GTP, Mr. Lúdvík S. Georgsson, Deputy Director, Ms. Thórhildur Ísberg, Mr. Markús A.G. Wilde and Mr. Ingimar Gudni Haraldsson for their tireless support and cooperation during our entire six month stay, making Iceland feel like home; to my supervisors, Ms. Annette Mortensen and Dr. Björn S. Hardarson: thank you very

much for your utmost support and guidance in the project throughout the entire period. I would also like to thank Dr. Hjalti Franzson, Mr. Gudmundur H. Gudfinnsson and the entire ISOR staff for assistance when analysing samples and during project work.

I would like to thank all the UNU Fellows 2012 for having a very wonderful time; it was very interesting. I hope to meet with you again in the near future.

I would also like to thank my employer, KenGen, for allowing me to come here and further my studies in geothermal energy. I would also like to take this opportunity to thank my family and wife for giving me the moral support, love, prayers and encouragement. To my daughter, Stephanie, who was born while I was here, it is a blessing to have you as my child.

Finally, I want to thank GOD for HIS blessings to us all.

REFERENCES

Agonga, O., 1992: *Geothermal geology: Stratigraphy and hydrothermal alteration of well OW-716, Olkaria geothermal area, Kenya*. UNU-GTP, Iceland, report 10, 44 pp.

Ambusso, W.J., and Ouma, P.A., 1991: Thermodynamic and permeability structure of Olkaria northeast field: Olkaria fault. *Geothermal Resource Council, Trans.*, 15, 237-242.

Baker, B.H., and Wohlenberg, J., 1971: Structural evolution of the Kenya Rift Valley. *Nature*, 229, 538-542.

Browne, P.R.L., 1978: Hydrothermal alteration in active geothermal fields. *Annual Reviews of Earth and Planetary Science*, 6, 229-250.

Browne, P.R.L., 1984: Subsurface stratigraphy and hydrothermal alteration of the eastern section of the Olkaria geothermal field, Kenya. *Proceedings of the 6th New Zealand Geothermal Workshop, Geothermal Institute, Auckland*, 33-41.

Clarke, M.C.G., Woodhall, D.G., Allen, D., and Darling G., 1990: *Geological, volcanological and hydrogeological controls on the occurrence of geothermal activity in the area surrounding Lake Naivasha, Kenya, with coloured 1:100 000 geological maps*. Ministry of Energy, Nairobi, 138 pp.

Davies, G.R., and MacDonald, R., 1987: Crustal influences in the petrogenesis of the Naivasha basalt-comendite complex: combined trace element and Sr-Nd-Pb isotope constraints. *J. Petrology*, 28, 1009-1031.

Franzson, H., 2011: *Borehole geology*. UNU-GTP, Iceland, unpublished lecture notes.

Haukwa, C.B., 1984: *Recent measurements within Olkaria East and West fields*. Kenya Power Co., Kenya, internal report, 13 pp.

Henley, R.W., and Ellis, A.J., 1983: Geothermal systems ancient and modern: a geochemical review. *Earth Science and Reviews*, 19, 1-50.

KenGen 1998: *Surface exploration of Kenya's geothermal resources in the Kenya Rift*. The Kenya Electricity Generating Company, Ltd, internal report, 84 pp.

Kenya Power Company, 1984: *Background report for scientific and technical review meeting*. Kenya Power Co., Ltd., internal report prepared by KRTA, 254 pp.

Lagat, J.K., 2004: *Geology, hydrothermal alteration and fluid inclusion studies of the Olkaria Domes geothermal field, Kenya*. University of Iceland, MSc thesis, UNU-GTP, Iceland, report 2, 71 pp.

MacDonald, R., Belkin, H.E., Fitton, J.G., Rogers, N.W., Nejbirt, K., Tindle, A.G., and Marshall, A.S., 2008: The roles of fractional crystallization, magma mixing, crystal mush remobilization and volatile-melt interactions in the genesis of a young basalt-peralkaline rhyolite suite, the Greater Olkaria volcanic complex, Kenya Rift Valley. *J. Petrology*, 49, 1515-1547.

MacDonald, R., Davies, G.R., Bliss, C.M., Leat, P.T., Bailey, D.K., and Smith, R.L., 1987: Geochemistry of high-silica rhyolites, Naivasha, Kenya Rift Valley. *J. Petrology*, 28, 979-1008.

MacDonald, R., and Scaillet, B., 2006: The central Kenya peralkaline province: Insights into the evolution of peralkaline salic magmas. *Lithos*, 91, 59-73.

Marshall, A.S., MacDonald, R., Rogers, N.W., Fitton, J.G., Tindle, A.G., Nejbirt, K., and Hinton, R.W., 2009: Fractionation of peralkaline silicic magmas: the Greater Olkaria volcanic complex, Kenya Rift Valley. *J. Petrology*, 50, 323-359.

McCall, 1967: *Geology of the Nakuru -Thomson's Falls - Lake Hannington area*. Kenya Geological Survey, report 70.

Mechie, J., Keller, G.R., Prodehl, C., Khan, M.A., and Gaciri, S.J., 1997: A model for the structure, composition and evolution of the Kenya Rift. *Tectonophysics*, 278, 95-118.

Muchemi, G.G., 1985: *Stratigraphy and hydrothermal alteration of well OW-601 Olkaria geothermal field, Kenya*. UNU-GTP, Iceland, report 6, 34 pp.

Mungania, J., 1992: *Geology of the Olkaria geothermal complex*. Kenya Power Co., Ltd, Kenya, internal report, 38 pp.

Naylor, W.I., 1972: *Geology of the Eburru and Olkaria prospects*. UN Geothermal Exploration Project, report.

Njue, M.L.M., 2010: Borehole geology and hydrothermal mineralisation of well HE-27, Hellisheidi geothermal field, SW-Iceland. Report 24 in: *Geothermal training in Iceland 2010*. UNU-GTP, Iceland, 463-492.

Ofwona, C., Omenda, P., Mariita, N., Wambugu, J., Mwawongo, G., and Kubo, B., 2006: Surface geothermal exploration of Korosi and Chepchuk prospects. KenGen internal report, 44 pp.

Omenda, P.A., 1994: The geological structure of the Olkaria west geothermal field, Kenya. *Stanford Geothermal Reservoir Engineering Workshop*, 19, 125-130.

Omenda, P.A., 1998: The geology and structural controls of the Olkaria geothermal system, Kenya. *Geothermics*, 27-1, 55-74.

Omenda, P.A., 2000: Anatectic origin for comendite in Olkaria geothermal field, Kenya Rift; Geochemical evidence for syenitic protholith. *Afr. J. Science & Technology, Science and Engineering Series*, 1, 39-47.

Pendon, R.R., 2006: *Borehole geology and hydrothermal mineralisation of well HE-22, Ölkelduháls field, Hengill area, SW-Iceland*. Report 17 in: *Geothermal Training in Iceland 2006*. UNU-GTP, Iceland, 357-390.

Reyes, A.G., 1990: Petrology of Philippine geothermal systems and the application of alteration mineralogy to their assessment. *J. Volc. Geoth. Res.*, 43, 279-309.

Reyes, A.G., 2000: *Petrology and mineral alteration in hydrothermal systems: from diagenesis to volcanic catastrophes*. UNU-GTP, Iceland, report 18-1998, 77 pp.

RockWare, 2007: *LogPlot program*. Rockware Inc.

Roedder, E., 1984: *Fluid inclusions*. Reviews in Mineralogy, 12, 664 pp.

Thomas, J., 2010: *Fairly simple geology exercises for students and their teachers*. Skidmore College, NY, website, www.skidmore.edu.

Thompson, A.O., and Dodson, R.G., 1963: *Geology of the Naivasha area, Kenya*. Kenya, Geological Survey, report 55.

Wheildon, J., Morgan, P., Williamson, K.H., Evans, T.T., and Swanberg, C.A., 1994: Heat flow in the Kenya Rift zone. *Tectonophysics*, 236, 131-149.

APPENDIX I: STRATIGRAPHY OF WELL OW-916

Depth	Rock description	Rock type	Alteration minerals
0-84	Brown to grey unconsolidated rock cuttings. Mixture of pumice, obsidian and rock fragments.	Pyroclastics	Clays Chabasite
84-266	Loss of circulation	-	-
266-306	Light brown porphyritic lava with quartz and sanidine phenocrysts. Cubic pyrite crystals also observed.	Crystalline tuff	Zeolites Pyrite, Oxides
306-344	Whitish crystalline lava. Flow banding is present with secondary quartz growing in vesicles. It is fractured.	Rhyolite	Pyrite, Illite Quartz
344-364	Loss of circulation	-	-
364-368	Whitish crystalline lava. Flow banding is present with secondary quartz growing in vesicles.	Rhyolite	Pyrite, Illite Quartz
368-382	Vesicular, homogeneous rock showing slight oxidation. Its light brown in colour with glass completely altered to green clays.	Scoria	Pyrite, Illite Oxides
382-402	Brownish fine grained heterogeneous formation with quartz and sanidine embedded in the groundmass.	Vitric tuff	Illite, Pyrite Oxides
402-414	Reddish brown fine grained slightly vesicular lava. Oxidation is quite high.	Tuff	Illite, Oxides Pyrite
414-444	Light brown heterogeneous rock showing slight alteration to green clays. Vesicles filled with clays.	Tuff	Oxides, Illite Calcite, Pyrite
444-450	Reddish brown fine grained highly oxidised rock	Tuff	Clays, Calcite
450-492	Dark brown heterogeneous rock containing lithic fragments in the groundmass.	Lithic tuff	Calcite Pyrite, Illite
492-498	Greenish fine grained rock showing high alteration. Low-temperature zeolite, thomsonite, observed	Tuff	Calcite, Illite Thomsonite
498-520	Light green vesicular rock with secondary quartz in vesicle. Appears scoreaceous.	Tuff	Quartz Calcite, Illite
520-544	Dark grey slightly porphyritic lava. Abundant calcite.	Basaltic intrusion	Calcite Illite

Depth	Rock description	Rock type	Alteration minerals
544-560	Dark brown fine grained rock containing lithic fragments and exhibits flow texture. First appearance of epidote in a vesicle at 556 m.	Welded tuff	Quartz, Illite Epidote
560-586	Green vesicular rock with quartz and clays infilling vesicles	Tuff	Quartz, Chlorite Calcite, Illite
586-628	Dark brown heterogeneous rock with lithic fragments in the ground-mass. Slight increase in oxidation.	Tuff	Quartz, Chlorite Illite, Pyrite
628-636	Reddish brown highly oxidised lava.	Tuff	Oxides, Clays
636-682	Light grey crystalline lava with secondary quartz in vesicles. Epidote infilling veins observed.	Trachyte	Quartz Epidote, Illite
682-692	Grey fine grained rock showing flow texture. Highly altered and is vesicular.	Tuff	Epidote, Calcite Pyrite, Illite
692-702	Light brown highly porphyritic lava with quartz and sanidine phenocrysts in the groundmass.	Rhyolite	Pyrite, Illite Oxides
702-724	Light grey fine grained rock with cubic pyrite crystals in the groundmass. Flow banding present.	Welded tuff	Pyrite Illite
724-742	Light brown slightly porphyritic with lithic fragments in the groundmass,	Rhyolitic tuff	Quartz, Illite Oxides
742-750	Light brown slightly porphyritic lava with quartz phenocrysts in the groundmass.	Rhyolite	Illite Pyrite
750-768	Brown porphyritic lava exhibiting flow texture. Highly altered and vesicular.	Rhyolite	Illite Pyrite
768-798	Light brown to light grey highly altered rock with quartz and sanidine phenocrysts in the groundmass.	Tuff	Quartz Clays, Illite
798-810	Light brown fine grained vesicular lava. Trachytic texture is observed and is highly altered with albitisation present.	Trachyte	Quartz, Illite Epidote
810-844	Light grey highly porphyritic lava showing flow banding. Vesicles filling of quartz and epidote observed.	Rhyolite	Quartz Epidote, Illite
844-850	Reddish brown highly oxidised rock.	Tuff	Clays
850-932	Grey to dark grey crystalline lava showing pyroxene phenocrysts in a plagioclase rich groundmass. High intensity of alteration observed.	Basalt	Prehnite, Epidote Wollastonite Quartz, Illite Calcite
932-950	Light grey fine grained rock. Appears glassy and glass is altered to green clays.	Scoria	Epidote Quartz
950-984	Reddish brown highly oxidised and altered rock.	Tuff	Clays, Oxides
984-1014	Light grey lava with quartz phenocrysts in the groundmass. It is fractured.	Rhyolite	Epidote Illite
1014-1092	Light grey porphyritic lava. Pyroxenes show alteration to actinolite.	Trachyte	Actinolite Wollastonite Illite
1092-1110	Reddish brown formation with lithic fragments in the groundmass. Highly altered and oxidised.	Tuff	Clays
1110-1124	Light brown fine grained porphyritic lava.	Trachyte	Epidote Illite
1124-1160	Light grey porphyritic massive lava. Show trachytic texture and sanidine phenocrysts altered to albite.	Trachyte	Actinolite Illite
1160-1168	Reddish brown rock with lithic fragments.	Tuff	Clays
1168-1186	Light grey porphyritic lava with pyroxenes showing alteration to actinolite.	Trachyte	Actinolite Wollastonite Epidote
1186-1190	Reddish brown oxidised rock.	Tuff	Clays
1190-1224	Light grey fine grained massive lava showing high intensity of alteration.	Trachyte	Actinolite Wollastonite Illite

Depth	Rock description	Rock type	Alteration minerals
1224-1240	Brown fine grained highly altered lava.	Tuff	Illite
1240-1270	Grey fine grained massive lava with veins and vesicles filled with epidote and quartz. Shows high alteration.	Trachyte	Epidote Quartz, Illite
1270-1286	Whitish silicic lava with quartz phenocrysts in the groundmass. Fractured.	Rhyolitic intrusion	Epidote Illite
1286-1294	Grey fine grained massive lava with veins and vesicles filled with epidote and quartz. Shows high alteration.	Trachyte	Epidote Quartz, Illite
1294-1304	Light grey to brown fine grained mixed lava. Highly altered and shows oxidation.	Mixed lava	Illite Epidote
1304-1340	Light grey vesicular lava. Appears fractured. Slightly oxidation. Altered to green clays.	Trachyte	Epidote Actinolite Quartz
1340-1348	Dark grey rock with lithic fragments exhibiting flow texture.	Welded tuff	Epidote, Illite
1348-1382	Light grey moderately altered lava with trachytic texture.	Trachyte	Epidote Actinolite, Illite
1382-1386	Dark grey fine grained rock.	Basaltic intrusion	Clays
1386-1400	Brown highly oxidised rock with secondary quartz in vesicles.	Tuff	Quartz, Illite
1400-1514	Light grey massive showing high intensity of alteration. Appears fractured and veined with actinolite replacing pyroxenes.	Trachyte	Actinolite Epidote Quartz, Illite
1514-1526	Light brown moderately porphyritic lava. Veining present with alteration intensity high.	Trachyte	Epidote Actinolite, Illite
1526-1556	Light grey fine grained lava with trachytic texture. Vein filling of white clays observed.	Trachyte	Actinolite Epidote Quartz, Illite
1556-1584	Light brown massive lava with vein fillings of actinolite, quartz and epidote. Appears fractured.	Trachyte	Actinolite Epidote Quartz, Illite
1584-1614	Light grey fine grained slightly porphyritic lava. Moderately altered.	Trachyte	Actinolite Epidote, Quartz
1614-1618	Dark grey fine grained relatively unaltered intrusive rock. Basaltic in origin.	Basaltic intrusion	Illite
1618-1662	Light grey to brown massive fine grained lava. Low intensity of alteration.	Trachyte	Illite
1662-1694	Light grey\brown lava. It is fractured and veined showing moderate to high intensity of alteration.	Trachyte	Actinolite Illite
1694-1754	Grey highly porphyritic lava. Fractured, veined and highly altered to green clays.	Trachyte	Actinolite Epidote, Illite
1754-1768	Light brown crystalline lava. Slightly porphyritic.	Trachyte	Actinolite Epidote, Illite
1768-1804	Light brown massive porphyritic lava. Fractured and moderately altered.	Trachyte	Illite
1804-1860	Light brown fine grained massive lava.	Trachyte	Illite, Epidote
1860-1870	Grey to brown mixed lava showing veining fillings of epidote.	Trachyte	Epidote Actinolite
1870-1914	Light grey fine grained lava with vein fillings of epidote and shows moderate intensity of alteration.	Trachyte	Epidote Actinolite, Illite
1914-1930	Light grey \brown massive feldspar rich porphyritic lava. Veined and moderately altered.	Trachyte	Epidote, Illite Actinolite
1930-1942	Loss of circulation	-	-
1942-1984	Light grey \brown massive feldspar rich porphyritic lava. Veined, fractured and moderately altered.	Trachyte	Epidote, Illite Actinolite
1984-2002	Loss of circulation	-	-

Depth	Rock description	Rock type	Alteration minerals
2002-2056	Light grey\brown massive crystalline lava.	Trachyte	Actinolite, Illite
2056-2084	Loss of circulation	-	-
2084-2110	Brown porphyritic fractured lava. Albitization is present.	Trachyte	Actinolite Epidote, Illite
2110-2162	Light grey crystalline lava. Vesicular and is highly altered.	Rhyolite	Epidote Actinolite, Illite
2162-2204	Light brown recrystallized lava. Veined and shows high intensity of alteration.	Rhyolite	Epidote Actinolite, Illite
2204-2216	Light grey heterogeneous lava.	Tuff	Epidote, Illite
2216-2226	Light grey crystalline lava. Vein fillings of epidote and clays observed.	Rhyolite	Actinolite Epidote, Illite
2226-2268	Light grey porphyritic lava. Fractured, veined and shows moderate intensity of alteration.	Trachyte	Actinolite Epidote
2268-2282	Loss of circulation	-	-
2282-2286	Light grey to white crystalline lava.	Rhyolite	Illite
2286-2324	Light brown medium-grained lava. Sanidine shows complete alteration to albite.	Trachyte	Epidote Actinolite, Illite
2324-2334	Light grey porphyritic lava. It's crystalline.	Rhyolite	Illite, Epidote
2334-2402	Loss of circulation	-	-
2402-2426	Light brown porphyritic lava. Shows moderate intensity of alteration to green clays.	Rhyolite	Quartz, Actinolite Epidote
2426-2450	Greenish fine grained lava. Slightly porphyritic, fractured and vein fillings of epidote observed.	Trachyte	Epidote, Actinolite Illite
2450-2564	Light grey slightly porphyritic massive lava showing high intensity of alteration.	Trachyte	Epidote Actinolite Illite
2564-2616	Light brown massive fine grained lava.	Trachyte	Epidote Actinolite, Illite
2616-2632	Mixed lava that's highly fractured and high intensity of alteration is present.	Mixed lava	Illite Epidote
2632-2662	Light brown porphyritic feldspar rich lava. Sanidine phenocrysts in the groundmass.	Trachyte	Epidote Actinolite, Illite
2662-2670	Light grey glassy rock showing alteration to green clays.	Rhyolitic intrusion	Illite
2670-2706	Light grey medium-grained lava with albitization present.	Trachyte	Illite, Epidote
2706-2726	Light grey porphyritic lava. It is veined and shows high intensity of alteration.	Trachyte	Illite Actinolite
2726-2752	Light brown fine grained veined lava.	Trachyte	Epidote Actinolite
2752-2792	Light grey porphyritic feldspar rich lava. Moderate intensity of alteration.	Trachyte	Actinolite Epidote, Illite
2792-2810	Loss of circulation	-	-
2810-2848	Grey slightly porphyritic massive lava. Moderately altered.	Trachyte	Actinolite, Illite
2848-2872	Whitish crystalline lava. Appears glassy and moderately altered to green clays.	Trachyte	Illite Actinolite
2872-2896	Grey porphyritic lava showing high alteration to green clays. Secondary quartz growing in vesicles.	Trachyte	Epidote Actinolite, Illite
2896-2952	Light grey fine grained moderately altered lava.	Trachyte	Epidote Actinolite
2952-2968	Whitish coarse grained syenitic intrusion	Syenite	Illite
2968-3000	Light grey light brown fine grained massive lava.	Trachyte	Illite, Epidote

APPENDIX II: Results of XRD analysis

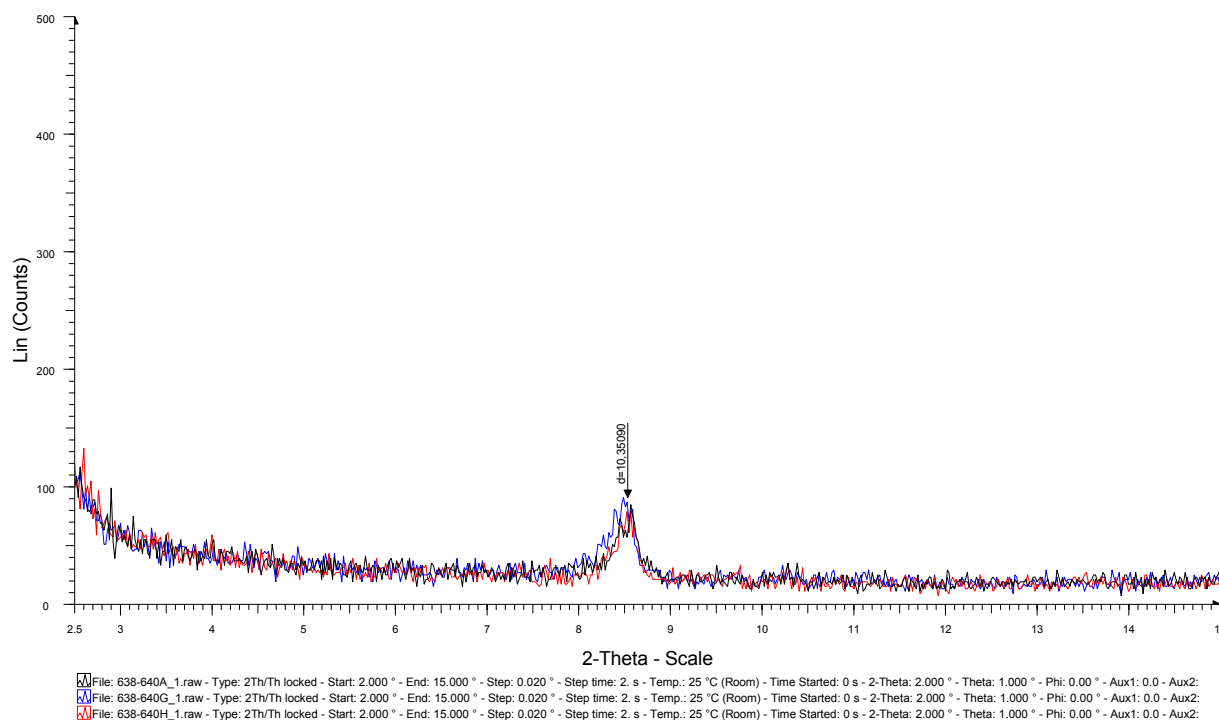


FIGURE 1: Well OW-16, XRD analysis of a sample from 638-640 m

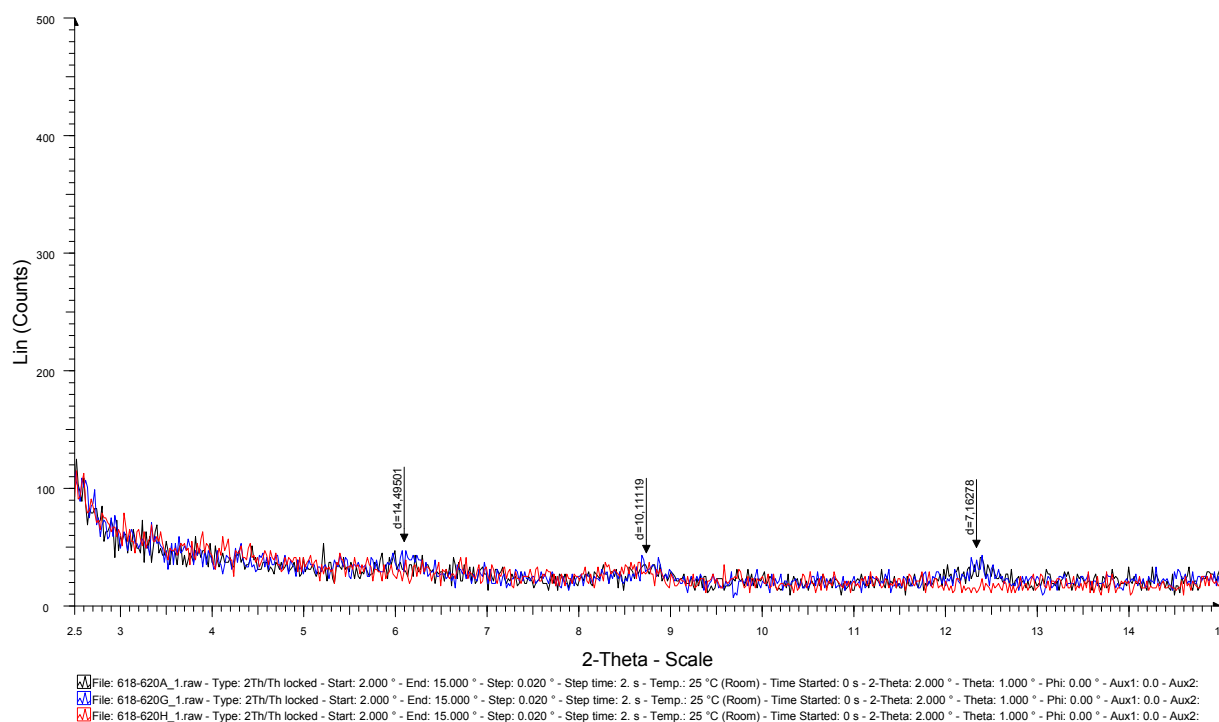


FIGURE 2: Well OW-16, XRD analysis of a sample from 618-620 m